Structurally diverse G-quadruplexes as the noncanonical nucleic acid drug target for living cell imaging and antibacterial study

Bo-Xin Zheng,[a,†] Jie Yu,[a,†] Wei Long,[b,†] Alan Siu-Lun Leung,[a] Ka Hin Chan [a] and Wing-Leung Wong [a,b,*]

[a] State Key Laboratory of Chemical Biology and Drug Discovery, Department of Applied Biology and Chemical Technology, The Hong Kong Polytechnic University, Hung Hom, Kowloon, Hong Kong SAR, China.

[b] The Hong Kong Polytechnic University Shenzhen Research Institute, Shenzhen 518057, P. R. China.

[†] The authors are contributed equally to this work

* Corresponding author

E-mail: wing.leung.wong@polyu.edu.hk

ORCID: 0000-0001-7191-7578

Abstract

The formation of G-quadruplex structures (G4s) *in vitro* from guanine (G)-rich nucleic acid sequences of DNA and RNA stabilized with monovalent cations, typically K^+ and Na^+, under physiological conditions, have been verified experimentally and some of them have high-resolution NMR or *X*-ray crystal structures; however, the biofunction of these special noncanonical secondary structures of nucleic acids has not been fully understood and their existence *in vivo* is still controversial at present. It is generally believed that the folding and unfolding of G4s *in vivo* is a transient process. Currently, accumulating evidence have shown that G4s may play a role in the regulation of certain important cellular functions including telomere maintenance, replication, transcription and translation. Therefore, both DNA and RNA G4s of human cancer hallmark genes are recognized as the potential anticancer drug target for the investigation in cancer biology, chemical biology and drug discovery. The relationship of the sequence, structure and stability of G4s, the interaction of G4s with small molecules, and insights into rational design of G4-selective binding ligands have been intensively studied over the decade. At present, some G4-ligands have achieved a new milestone and successfully enter human clinical trials for anticancer therapy. Over the past decades, numerous efforts have been devoted in anticancer; however, the study of G4s on molecular recognition and live cell imaging, antibacterial and antibiofilm against antibiotic resistance are obviously underexplored. The recent advances of G4-ligands in these areas are thus selected and discussed concentratedly in this article in order to shed light on the emerging role of

G4s in chemical biology and therapeutic prospects against bacterial infections. In addition, the recently published molecular scaffolds for designing small ligands selectively targeting G4s in live cell imaging, bacterial biofilm imaging, and antibacterial study are discussed. Furthermore, a number of underexplored G4-targets from the cytoplasmic membrane-associated DNA, the conserved promoter region of *K. pneumoniae* genomes, the RNA G4-sites in the transcriptome of *E. coli* and *P. aeruginosa*, and the mRNA G4-sites in the sequence for encoding the vital bacterial FtsZ protein are highlighted to be further explored in G4-drug development against human diseases.

1. Introduction

The guanine(G)-rich nucleic acid sequence of DNA and RNA stabilized with metal ions, typically potassium and sodium ions, under physiological conditions, is found showing high propensity to fold into a stacked tetrad structure in which four guanines are linked by Hoogsteen base-pairs in a co-planar manner.[1-3] This special form of interaction and conformation is different from the traditional helical double-stranded DNA structure formed in canonical Watson–Crick base pairing (**Figure 1 A-B**). These unique noncanonical secondary structures are rigid and thermodynamically more stable upon formation through the self-association of guanine bases in the sequence and are usually termed as G-quadruplex (G4).[4] The G-rich nucleic acid sequences are commonly found in many living systems, such as the plant, virus, bacteria, animal and human,[5-7] and can form countless and highly diverse G4-structures *in vitro* depending on their sequences. Recent results reveal that there are more than 700,000 G4-forming sequences found in the human genome.[8] Interestingly, these G-rich sequences are not simply distributed randomly in human cells. In addition, the putative G4-forming sequences are not found in most of small ncRNA families.[9] On the contrary, they are found mostly concentrated on certain locations of the gene including in telomeres as a repeated unit, replication initiation sites, promoter regions of oncogenes such as *MYC*, *KIT* and *RAS* genes (*KRAS, NRAS, HRAS*), 5'- and 3'-untranslated regions of mRNA, splicing junction of mRNA, the long ncRNA, and mitochondrial genome.[10-12]

The biofunction of G4s has not been fully understood currently. It is generally believed that G4s may play crucial roles in the regulation of several important cellular functions including telomere maintenance, replication, transcription and translation, which have been investigated with computational predictions and experimental studies in recent years.[13-26] Despite numerous experimental evidences, including high-resolution NMR[27-29] and *X*-ray crystal structures,[30-32] G4-selective molecular fluorescent sensors,[33-40] G4-resolving enzymes such as helicases, and G4-specific antibodies[41, 42] such as BG4, HF1, HF2 and 1H6, strongly support that G4s can be formed *in vitro* under certain conditions, whether these structures really existing in live cells is still a controversial question.[43, 44] One of the uncertainties cannot be easily ruled out is that the

intracellular observable G4s formed could be probably induced by molecules such as G4-binding ligands and proteins at the site. It is reported that DNA G4-formation could be in response to remote downstream transcription activity.[45] It is also argued that the *in vivo* G4s such as RNA G4s in human cells may exist transiently during their dynamic process of folding and unfolding.[46] Nonetheless, since the discovery of biologically relevant G4s in the eukaryotic chromosomal telomeric DNA consist of the repeated sequence TTAGGG,[47] the finding has illuminated an unprecedented role of DNA in biology.[48] The 2009 Nobel Prize in Physiology or Medicine was awarded for the discovery of telomeres and telomerase.[49, 50] So far, numerous structural information about DNA G4s have been reported and that shows a great conformational diversity of G4s, which are recognized as the potential drug target against many human diseases,[51-56] particularly cancers.[57-67] The relationship of the sequence, structure and stability of G4s, their interactions with small molecules *in vitro* and *in vivo*, and insights into rational design of G4-selective binding ligands have been well documented and intensively reviewed over the decade.[68, 69]

The therapeutic prospects of G4s against human diseases have been a hot research field over the past decades. A rough survey performed for the period of 2010–2022 based on the database of SciFinder® shows that there are more than 12,000 research articles published on the topic of G4s. Among these publications, the majority is closely related to drug discovery against human diseases, which include mainly anticancer (~2245 papers), anti-neurological diseases (~255 papers), antivirus (~144 papers), antibacterial (~52 papers) and antibiofilm (~11 papers). Obviously, the study in the field of antibacterial and antibiofilm is relatively under investigated compared to other fields. Due to limited space and avoiding significant overlapping with the previously reviewed contents targeting G4s, only the research focused on fluorescent live cell imaging, antibacterial and antibiofilm is discussed concentratedly in this review in order to shed light on the emerging roles of G4s in chemical biology and therapeutic prospects against bacterial infections resistant to antibiotics. The contents summarized and discussed herein could be complementary to the recently published reviews on the topic of G-quadruplex.

<<Figure 1>>

2. Bioinformatics and biological functions of G4-structures

In addition to the well-known canonical double-stranded B-DNA, many G-rich nucleic acid sequences in the genome may form thermodynamically stable G4s *in vitro* and may exist transiently *in vivo* as non-canonical conformations. G4s are stacked with two or more planar G-tetrads (or termed G-quartets) in which four guanines are linked together by Hoogsteen-type hydrogen bonding. G4s usually complex with monovalent cations (typically K^+ and Na^+) to further stabilize the structure (**Figure 1C-D**). The potential of a G-rich sequence in forming G4s is predictable with

computational algorithms. Currently, a consensus sequence motif, 5'–$G_{\geq 3}N_{1-7}G_{\geq 3}N_{1-7}G_{\geq 3}N_{1-7}G_{\geq 3}$–3', has been used to identify putative G4s from DNA and RNA sequences. A recent review discussed the latest technique for the identification of G4s for a primary sequence.[70] Based on the extensive biophysical and structural studies have been reported thus far, it is known that G4-structures are highly diverse. Their conformations mainly depend on the number of stacked G-tetrads, the length of interconnecting loops and the sequence. In addition, both the strand orientation during the folding process to form G4s and the nature of the cation present in the central ion channel are crucial factors. In general, the *in vitro* secondary structure of G4s upon formation are more stable than their corresponding primary sequence. It is experimentally supported by many melting studies such as the fluorescence resonance energy transfer (FRET) melting and circular dichroism (CD) thermal denaturation assays.

Most biological studies reported thus far are focused on the monomeric G4. It is noteworthy to highlight that G4s formed *in vitro* from DNA or RNA strands can be monomeric and multimeric. It is also known that human DNA sequences of c-MYC promoter, hTERT core promoter and telomere are able to form multimeric G4s. The difference of monomeric and multimeric G4s has been discussed and reviewed recently.[71, 72] The G-tetrads of a monomeric G4 can fold into three typical topologies including parallel, antiparallel and hybrid with the loops adopting different conformations: propeller, lateral and diagonal.[3] Multimeric G4s can be assembled *in vitro* by inter- or intra-molecular G4 subunits. The intermolecular G4 forms from the G-tetrads, which accommodate guanine residues that come from separate nucleic acid strands. The dimeric, trimeric and tetrameric structures are found in intermolecular G4s. The strands taking part in these multimeric G4s formation may exclusively come from DNA strands or from both DNA and RNA strands that result in the formation of a DNA:RNA hybrid structure. On the contrary, multimeric intramolecular G4s are established on the same nucleic acid strand via the stacking of monomeric G4 subunits, which are influenced by G4 topology and loop orientation. However, the antiparallel topology is not favorable for the stacking of multiple G4s.[73] Intramolecular G4s formed from promoter genes usually fold into parallel topology (**Figure 1E**).[74]

Despite whether G4-structures really existing *in vivo* is still an open question, accumulating evidence have established clear links between G4s and many human diseases. The field has attracted great interest over the past decades.[68, 69, 75] Moreover, G4-forming sequences in cells are found highly localized only at certain regions of the gene that regulates genome functions. This observation may imply that G4s may possibly implicate in a range of biological processes. Since the first discovery of biologically relevant G4s in telomeres of eukaryotic chromosomes, the possible biological role of G4s in cancer has been focused on their regulation of telomere maintenance, gene expression, genome duplication, and genomic and epigenetic stability (**Figure**

2A).[15, 16, 25, 76] Thus, these key genome functions make G4s a potential therapeutic target against human cancers. In addition, the altered expressions of G4s in cancer-promoting genes are recognized as hallmarks of cancer. Experimental results have shown a higher presence of G4s in cancer states compared with normal states,[77] which may favor G4s as the molecular drug target for anticancer therapy. The development of G4-binding ligands such as **TMPyP4** that induces a global increase of native G4s at promoters[78] to induce and/or stabilize intracellular G4s is able to repress the expression of G4s in cancer hallmark genes.[66, 68, 79-81]

In general, G4-structures share a common feature of stacked G-tetrads as the basic motif that is a square-planar-like structure and is favorable for π-π interaction with planar small-molecules;[3, 82-84] however, intramolecular G4s could show great conformational diversity in folding topology, loop conformation and capping structures.[85] Interestingly, different categories of G4s in cancer cells were found associated with different biological functions including self-sufficiency for growth signals, insensitivity to anti-growth signals, evasion of apoptosis, sustained angiogenesis, limitless replicative potential, and tissue invasion and metastasis (**Figure 2B**).[86, 87] Because of G4s associated with these essential cellular functions, it is thus generally accepted that G4s are the potential therapeutic drug target for cancer therapy.[88] Nonetheless, the development of target-specific G4-ligands to achieve cytotoxic potency against the massive double-stranded DNA, proteins and other intracellular substrates *in vivo* remains a great challenge in drug discovery.

<<Figure 2>>

3. Fluorescent G4-selective ligands for molecular recognition and sensing in live cells

During the past decade, many research work (over 300 papers) have been published on the development of G4-selective fluorescent sensors for *in vitro* and *in vivo* study. These molecular recognition and sensing systems developed can provide important insights into the creative design of G4-specific drugs. Small-molecule based fluorescent G4-ligands have been demonstrated to be a useful tool for monitoring of the complicated dynamic process of G4s formed from DNA or RNA, and their cellular locations in living cells,[39, 40, 89-93] which can offer real-time information of the intracellular G4s for chemical biology study and drug discovery.[94] A number of recent reviews has been published and concluded the recent progress on fluorescent sensing of G4s in live human cancer cells.[35, 95-99] In addition to the organic molecular fluorescent probes, the real-time sensing and monitoring of cellular G4s can be achieved with highly selective synthetic fluorescent oligonucleotides or proteins.[100-102] These work are not discussed herein due to out of the focus of the present study.

G4-structures are highly diverse and subtle. Despite molecular simulations and docking studies may predict their structures, there is no clear rules or guidelines that can be followed to design a

ligand specifically binding to a desired G4-target. Nevertheless, to design ligands with high selectivity to a certain category of G4s is achievable. To enhance π-π interaction via stacking with the planar G-tetrad at two ends of the G4-structure, the ligands are usually designed to have a planar or a rotatable co-planar core molecular fragment. Another common feature of G4-ligand is positively charged, which can establish electrostatic interactions with the negatively charged guanine carbonyl oxygens at the center to enhance affinity and stabilize the complex formed. Some representative G4-ligands that include but not limited to **CX-3543**, **CX-5461**, **GQC-05**,[103] **Mitoxantrone**,[104] **RHPS4**,[105] **Berberine**,[106, 107] **BRACO19**,[108] **TMPyP4**,[109] **Phen-DC3**,[110] **Pyrodostatin** (**PDS**),[111, 112] and **Thioflavin T**[113-115] are shown in **Figure 3**.

<<Figure 3>>

In attempts to probe the crucial factors in rational design of G4-selective ligands, our group has developed several ligand systems. We found that, apart from adopting a planar core molecular fragment to construct G4-ligands, the overall molecular size,[116] symmetry,[117, 118] flexibility,[83] and the character of terminal groups[119-122] may affect the *in vitro* selective of the ligand toward G4-structures against RNA, single- and double-stranded DNA. Our study suggests that some small-sized molecular scaffolds including benzothiazole-benzofuroquinolinium,[123, 124] benzothiazole-indolium,[125] 1-methylquinolinium,[126] thiazole orange[81, 84, 127] and benzo[*e*]indole[128] are good molecular fragments for the design of fluorescent G4-ligands to achieve high discrimination ability, sensitivity and quantum yield targeting certain type of G4s for *in vitro* sensing and live cell imaging. In the design of G4-ligands, the molecular symmetry of G4-ligands is rarely discussed in literature. Our study with a series of C_1-, C_2- and C_3-symmetric pyridinium conjugates as fluorescent G4-probes with different styrene-like terminal groups demonstrates that the C_2-symmetric probe with indolyl-groups substituted at the terminal offers the best selectivity and sensitivity toward G4-DNA, particularly targeting telo21 (equilibrium binding constant, K_{eq}=2.17×10^5 M^{-1}; limit of detection (LOD)=33 nM) (**Figure 4A**). The finding indicates that both molecular symmetry and the nature of terminal groups may be crucial factors for considering on the development of G4-selective ligands.

A new molecular design based on the 1-methylquinolinium scaffold to develop near-infrared (NIR) fluorescence probe was reported.[126] In this G4-ligand system, an analogue integrated 1-methylquinolinium with both dimethylamino-styryl and methylpiperidyl substituent groups (**Figure 4B: A3**) showed intensive red fluorescence (λ_{ex}=498, λ_{em}=610) with a large Stokes shift (112 nm) and a high quantum yield (Φ_f=0.56) upon interacting with G4-DNAs of KRAS, HRAS, c-MYC and telomere *in vitro*, while the non-G4 DNA substrates showed much less effective interaction signal. It was found that the integration of a rotatable terminal amino group to 1-methylquinolinium scaffold resulted in high selective toward G4-DNA substrates.[126] In addition,

the immunofluorescence assays using a G4-specific antibody (BG4) to colocalize with **A3** in PC3 cells suggest that **A3** is G4-selective and can be used for visualizing G4-DNA in live cells. In particular, targeting c-MYC pu27 G4-DNA, a LOD obtained was found down to 4.0 nM. Furthermore, a small-sized G4 fluorescent probe, **BZT-Indolium** (molecular mass=321 g/mol) synthesized with a benzothiazole-indolium scaffold, was demonstrated as a highly selective and photostable sensor for live cell imaging targeting the c-MYC promoter G4-DNA. This ligand was able to discriminate c-MYC G4s from other classes of G4s such as those from telomere (**Figure 4C**). The ligand also inhibits the amplification of the c-MYC G4-sequence by Taq DNA polymerase and down-regulates oncogene c-MYC expression in HeLa cancer cells.[125]

<<Figure 4>>

Structural modification based on a non-selective thiazole orange scaffold can also make the ligand achieve high selectivity toward c-MYC or telomeric G4-DNA structures. Attempts to discriminate these two classes of G4s, we have recently reported a new approach in the design of small molecules by molecular engineering thiazole orange with extended functional groups. The new ligand design allows two-directional and multi-site interactions with the flanking residues and loops of a G4-motif for achieving better selectivity.[81] This structural feature renders the G4-ligand showing higher selectivity toward a certain class of G4s than other nucleic acid structures. We identified two ligands, **Figure 5**: **2** and **3**, bearing different terminal substituent groups, that showed obviously different selectivity toward promoter and telomeric G4s. The study demonstrates that **2** preferentially binds to telomeric G4, while **3** has higher selective toward c-MYC G4. Molecular docking study using AutoDock Vina predicted a different mode of interactions for the two ligands with a c-MYC G4-structure (PDB 2MGN)[129] and revealed that **3** possessed two terminal phenyl rings that established loop interactions. The ligand system of **3** demonstrates that multi-site interactions including π–π stacking, hydrogen bonding and loop interactions may rigidify the π–conjugation system of **3** and thus the ligand is able to provide excellent structural discrimination between c-MYC and telomeric G4-structures.

<<Figure 5>>

RNA G4s are multifaceted and their intracellular existing is also controversial. Despite RNA G4s are recognized as the important drug target, the understanding on their structures and biological functions is still limited at present.[56, 130-135] Currently, a number of fluorescent probes have been developed for imaging of cellular RNA,[136-141] however, molecular fluorescent sensors targeting RNA G4s are rarely found in literature. There are only few fluorescent ligand systems recognizing RNA G4s reported and demonstrated in live cell imaging (**Figure 6**).[142-146] The feature of the RNA G4-selective probes of **CyT**, **QUMA-1** and **N-TASQ** has been reviewed recently.[95] Compared to DNA G4s, fluorescent probes targeting RNA G4s remain extremely underexplored although both

nucleic acid targets may have the same significance in drug discovery against human diseases such as cancers. The limited structural information of RNA G4s, such as the crystal structures, either natural or artificial, may be one of the hurdles that largely increase the difficulty in rational design of selective fluorescent probes targeting RNA G4s. At present, there are about 9 unique *X*-ray crystal structures deposited in Protein Data Bank (PDB).[147] To increase the understanding on the structural property of RNA G4s, apart from *X*-ray crystallography, high-resolution NMR spectroscopy and computational methods may be an indispensable tool.

BEDO-3 is the most recently reported fluorescent small molecule selectively targeting RNA G4s in live cells.[145] The probe is designed to bear an extended aromatic ring (phenyl *versus* naphthyl) and amino side chain that are able to interact with both the G-quartet and phosphate backbone. By comparing the structural property of its analogues, the naphthothiazole scaffold of **BEDO-3** was found a critical unit that rendered a high binding affinity and specificity of the molecule toward RNA G4s. However, the extended aromatic ring from phenyl to naphthyl does not push a significant redshift in the excitation and emission wavelength of the ligand (λ_{ex}=480 nm, λ_{em}=540 nm) but it gives much higher quantum yields (Φ_f=0.374) upon interacting with TERRA G4-structure. Competition assay and BG4 colocalization study also indicate that **BEDO-3** is an RNA G4-selective probe. The LOD value of the probe targeting FMR1 in buffer and cell lysate solution was found to be 0.43 nM and 1.08 nM, respectively. Its LOD is approximately 5-fold better than that of **QUMA-1**. Moreover, live cell imaging of RNA G4s with **BEDO-3** in HeLa cells was demonstrated. The probe is able to monitor or track the real-time motion of the RNA target in the cell (**Figure 6 A-F**). Nevertheless, the mobility analysis of intracellular foci of **BEDO-3** does not provide information on the dynamic folding/unfolding of RNA G4s in live cells.

<<Figure 6>>

Mitochondria in cells are the home of cellular metabolisms. Mitochondrial G4s also play vital roles in regulating mitochondrial gene functions. For example, an association between human mitochondrial DNA (mtDNA) deletion breakpoint locations and G4-forming sequences was reported.[148] Moreover, RNA G4s may play roles in altering mitochondrial replication, transcription and translation.[10] The study on the emerging roles of G4s in mitochondria has been discussed comprehensively in recent reviews.[11, 149] Despite several fluorescent probes selectively recognizing and imaging mtDNA G4s have been reported, compared to nuclear DNA G4s, the ligand system developed thus far is very limited. The reported fluorescent ligands with high selectivity toward mtDNA G4s against other types of G4s and nucleic acid structures were summarized in **Figure 7** for structural comparison. The analysis of these molecular scaffolds may provide meaningful insights into designing target-specific mtDNA G4-binding ligands for chemical biology study and drug discovery against mitochondrial diseases.[150, 151]

<<Figure 7>>

Most mtDNA G4-selective fluorescent sensing systems with organic-based small molecules were published in the past three years (2020–2022), indicating that mtDNA G4s are becoming an attractive molecular target. It is expected that more exciting information and understanding on their cellular biofunctions could be discovered in the near future. From these mtDNA G4-selective ligands reported recently (**Figure 7**), it is noteworthy that some molecular scaffolds including benzothiazole, coumarin, quinazolinone, thiazole orange, indole, benzoindole, carbazole, triphenylamine, triphenylphosphine and tetraphenylethylene are frequently utilized in the design of mtDNA G4-probes. This may give a hint that these molecular fragments could have high propensity entering the mitochondria and then bind to mtDNA G4s. These new ligand systems may give an idea to design organelle-specific fluorescent probes or molecular carriers because the topic of organelle-specific drug targeting encounters many challenges, particularly targeting mitochondria for pro-apoptotic cancer therapy and lysosomes for enzyme therapy for lysosomal storage diseases.[152, 153]

The ligand **SPN** integrated with the scaffold of benzothiazole and triphenylamine was demonstrated as a mtDNA G4s sensor achieving high fluorescent sensitivity (λ_{ex}=540 nm, λ_{em}=640 nm) and stability toward mtDNA G4s with a LOD as low as 0.89 nM (**Figure 8A**). The fluorescence quantum yield of **SPN** (4-10%) is not high but the ligand could highly localize in mitochondria allowing recognition and monitoring of mtDNA G4s in live HeLa cells. In addition, from the confocal fluorescence imaging of mitochondria, the fluorescence intensity of the ligand in cancer cells was generally found significantly stronger than that in non-cancerous cells. This special discrimination property of **SPN** may suggest a potential application for cancer diagnosis.[154] Furthermore, the cytotoxicity of **SPN** against HUVEC and HeLa cells was examined and the IC_{50} was higher than 20 μM regardless of short-term or long-term incubation with the cells. The result indicates that the ligand has moderate toxicity.

Another two ligands, **AMTC** and **DMTOY**, with a similar molecular structure constructed by connecting two benzothiazole scaffolds via a conjugated methylene or propylene bridge were also reported to be mtDNA G4-selective.[155, 156] **AMTC** in the form of face-to-face stacked dimer are non-fluorescent because the dimer has two exciton states that only allow the transition to the higher energy exciton state. Nonetheless, **AMTC** monomer emits fluorescence (λ_{ex}=555 nm, λ_{em}=583 nm) but its fluorescence intensity is very weak due to the intramolecular torsional motion of the C–C bond in the polymethine chain. The delivery mechanism of **AMTC** into the mitochondria was found membrane potential dependent. Its analogue ligand **DMOTY** monomer shows an emission maximum near 520 nm (λ_{ex}=430 nm). The cellular localization of both ligands was demonstrated in mitochondria of live HeLa and MCF-7 cells but there was no cytotoxicity information of the

ligands given. MitoTracker was utilized for colocalization study with the ligands (**Figure 8B-C**). In addition, the selectivity of these ligands targeting mitochondrial G4s was illustrated by intracellular competition studies with RHPS4 and **BRACO19**.

Fluorescent ligands utilizing coumarin, quinazolinone and thiazole orange scaffolds were also reported for the design and synthesis of mtDNA G4-selective sensors. A crescent-shaped ligand **NCT** is constructed with a coumarin and a thiazole orange unit through a conjugated ethylene bridge. This molecular scaffold combination offers a NIR fluorescence emission (λ_{ex}=488 nm, λ_{em}=650 nm) upon the ligand interacted with mtDNA G4s *in vitro* and in live HeLa cells.[157] The LOD of the ligand toward CM22 (a mtDNA G4) determined was 3.1 nM, indicating the high sensitivity of the ligand. Fluorescence lifetime measurements performed for **NCT** binding to various DNAs in buffer was found generally increased for G4-DNAs (**NCT**-CM22 complex=1.3 ns) compared to non-G4 DNA substrates (single- and double-stranded DNAs: 0.8–0.9 ns) and free ligand (0.4 ns). The colocalization experiment shows that **NCT** is mainly localized in mitochondria but not in nucleus. It could be due to the poor nuclear membrane permeability of the ligand. **NCT** co-staining with MitoTracker green demonstrated a highly overlapped area in HeLa cells (**Figure 8D**). The cell-based toxicity assay shows that **NCT** has relatively high cytotoxicity against HeLa cells (incubated with **NCT** at 8 μM for 24 h, the cell viability was about 50%; IC_{50} was not given).

The monomeric form of a coumarin-quinazolinone conjugate, **CQ**, shows bright fluorescence in organic solvents while it exhibits an aggregation-caused quenching effect in aqueous solution due to self-assembly aggregation.[158] **CQ** is also found selectively binding to G4-DNA and then generates fluorescence via aggregation–disaggregation switching in live HepG2 cells (λ_{ex}=488 nm, λ_{em}=500–550 nm). The intracellular colocalization study of **CQ** with MitoTracker Red CMXRos and LysoTracker Red DND-99 demonstrates that **CQ** specifically targets mitochondria (**Figure 8E**). Moreover, the fluorescence of **CQ** is found enhanced upon interacted with parallel or hybrid G4s including mtDNA G4-sequences such as PMPS, HRCC, and KSS *in vitro*. The interaction of **CQ** with mtDNA G4s in live cells was demonstrated by using a displacement assay in which the **CQ** bound to G4s was replaced with Thioflavin T (**ThT**). However, **ThT**, similar to **TO** dye, is a non-specific fluorescent probe that could interplay with in various DNA structures in three different binding modes including intercalation, external binding and binding inside DNA cavities.[159] Therefore, the intracellular binding target of **CQ** in mitochondria may be not conclusive.

To enhance the organelle specificity of the ligand, a lipophilic and cationic triphenylphosphonium (TPP) moiety[160] that is known to drive the accumulation of organic molecules in mitochondria in response to the membrane potential was integrated into the design of mtDNA G4-selective ligands. **MitoISCH** is synthesized by incorporating TPP with a coumarin-quinazolinone conjugate and is demonstrated as a mtDNA G4-selective fluorescent probe (λ_{ex}=560

nm, λ_{em}=650 nm).[161] The tagging of a TPP group to thiazole orange and coumarin 110 dye was also performed as a control. Despite these two control dyes were also found concentrated in mitochondria of live HeLa cells, they were generally much less selective targeting mtDNA G4s in live cell imaging experiments. It is probably due to both thiazole orange and coumarin 110 dyes are non-specific toward G4-structures. The cellular location of **MitoISCH** at mitochondria is verified with the colocalization study using MitoTracker Green and LysoTracker Green in live HeLa cells (**Figure 8F**). To characterize the specificity of **MitoISCH** targeting mtDNA G4s, competition assays with **MitoISCH** and RHPS4 (a G4-selective ligand) were conducted in HeLa cells. The results suggest that **MitoISCH** is selective to mtDNA G4s. The cytotoxicity of the ligand was examined and the IC_{50} against HeLa cells was found greater than 20 μM for 3 h treatment. In addition, the ligand was utilized to investigate the relationship between mtDNA G4 formation and glycolysis levels in HepG2 cells. The results reveal that an upregulation of glycolysis by hypoxia may cause an increase in the quantity of intracellular mtDNA G4s. The probe may provide a useful chemical tool for investigating the role of mtDNA G4s in cancer cell metabolism.

We have recent developed a mitochondria-specific fluorescent ligand with the use of a planar molecular scaffold of benzo-indole to conjugate with a rotatable *p*-substituted styrene moiety via an ethylene bridge.[128] The ligand **BYM** was found selectively binding to mtDNA G4s both *in vitro* and *in cellulo* and generates red emission signal (λ_{ex}=530 nm, λ_{em}=615 nm, Φ_f=0.389). The LOD of **BYM** targeting mtDNA G4 (mt6363) determined was 1.52 nM. **BYM** also shows higher binding preference toward parallel G4s than anti-parallel and hybrid topologies. Confocal images of the colocalization study with MitoLiteTM-Blue and Lyso-Tracker Green show that the ligand is localized in mitochondria but not nucleus (**Figure 8G**). The study of intracellular competition with **BRACO19** and dimethyl sulfate (DMS) assays in live HeLa cells demonstrate that the cellular target of **BYM** most likely is a G4-structure. **BYM** also exhibits a much higher photostability than MitoTracker Red CMXRos. In addition, **BYM** at 5-10 μM exhibits almost no cytotoxicity against a number of human cancer cells and non-cancerous cells. Furthermore, the real-time immunofluorescent colocalization of the autophagosome protein LC3 and **BYM** in live HeLa cells was demonstrated. The results suggest that the ligand is a non-toxic and useful chemical tool for live cell imaging and mitophagy monitoring study with minimum interference on the live cell activity.

An indole-based NIR fluorescent ligand **TAIN-2** integrated with a triphenylamine scaffold (a small scaffold similar to TPP) via an ethylene bridge was reported for G4s visualization and stabilization *in vitro* and in live cancer cells.[162] In the ligand design, the integration of two indolyl groups to triphenylamine (**TAIN-2**) exhibits better fluorescence enhancement than its analogue just with one indolyl group upon interacted with G4s. **TAIN-2** also gives longer excitation and emission

wavelength (λ_{ex}=550 nm, λ_{em}=740 nm) than its analogue. The confocal imaging study with **TAIN-2** in MDA-MB-231 cells indicates that the ligand is mostly localized in cytoplasm. However, the colocalization study of the ligand with MitoTracker and Lyso-Tracker was not performed to demonstrate mitochondria-specificity. Nonetheless, the intracellular G4-targets of **TAIN-2** was supported with PDS competition experiments and DMS assays in MDA-MB-231 cells. Moreover, **TAIN-2** is able to cause DNA damage and induce G2/M cell cycle arrest. The proliferation of MDA-MB-231 cells was inhibited by the ligand with IC_{50} values of 6.3 μM, 5.7 μM and 4.2 μM after the treatment for 24 h, 48 h and 72 h. The results indicate that the ligand is toxic against MDA-MB-231 cells.

Another example of NIR fluorescent ligand **IZIN-1** is developed based on the indole-triphenylamine scaffold. The ligand is demonstrated as a mitochondrion-targeting AIE luminogen and generates NIR fluorescence upon interacting with G4s in live A549 cells (λ_{ex}=538 nm, λ_{em}=660 nm).[163] **IZIN-1** shows higher binding preference toward mtDNA 4G (mt6363) than some other types of G4-structures examined. However, no information on the binding affinity and LOD was given. **IZIN-1** was mainly accumulated in mitochondria evidenced by colocalization with MitoTracker™ Green in live A549 cells (**Figure 8H**). Its cellular G4-target was also demonstrated with PDS competition assays. The robustness against photo-bleaching and cytotoxicity of the ligand have not been investigated.

Flavylium scaffold is also adopted for the design and synthesis of mitochondria-targeting ligands. A substituted flavylium-dimer **FLV1** coupled with a rigid but rotatable methylene bridge was reported as a mtDNA G4-selective NIR fluorescent ligand (λ_{ex}=660 nm, λ_{em}=700 nm).[164] The use of a propylene bridge of the ligand can make the absorption and emission wavelength further red shift. Live cell imaging study with **FLV1** in HeLa, A549 and SHSY5Y cells indicated that the ligand was localized in cytoplasm. Colocalization study with LysoTracker blue and MitoTracker green in the cells shows that **FLV1** is mitochondria-specific (**Figure 8I**). It was found that the delocalized positive charge of **FLV1** likely facilitated its diffusion into mitochondrial membrane but independent of mitochondrial membrane potential. Despite six mtDNA G4-forming sequences were verified to show interactions with **FLV1** *in vitro*, the intracellular interaction of the ligand with mtDNA G4 targets was not investigated.

The integration of thiazole orange and tetraphenylethylene scaffolds is applied in the design of mtDNA G4-selective fluorescent ligands. The two molecular fragments were connected via a conjugated ethylene bridge to synthesize **TPE-mTO** as a mitochondrial targeting fluorescent probe that has a mechanism of aggregation induced emission because the tagged tetraphenylethylene scaffold can act as an AIEgen.[165] The LOD of **TPE-mTO** toward CM22 was 4.1 nM. Moreover, **TPE-mTO** interacts with different types of G4s and generates fluorescence enhancement (λ_{ex}=488

nm, λ_{em}=530 nm). Despite the ligand exhibits certain degree of preference toward CM22 (a parallel G4), it does not discriminate well among the G4 substrates tested in the study. Intracellular colocalization study of **TPE-mTO** with MitoTracker Deep Red in A549 cells indicates that the ligand is mitochondrial targeting (**Figure 8J**). However, the G4 identity stained by the ligand in mitochondria has not been further verified.

A carbazole-based ligand **BMVC-12C-P**, a known fluorescent anticancer agent, was reported targeting mtDNA G4s in cancer cells. The study demonstrated the use of fluorescent life time imaging microscopy (FLIM) as a tool to visualize the localization of G4s in live cells because the G4-ligand show a longer fluorescence decay time (≥2.4 ns) when interacted with G4s than that of calf thymus DNA (~1.2 ns).[166] In addition, **BMVC-12C-P** was found accumulated primarily in the mitochondria of HeLa cells. Interestingly, it is less accumulated in normal cells (MRC-5). The live cell confocal images also show that the ligand is well colocalized with MitoTracker red in live HeLa cells (**Figure 8K**). Moreover, the cellular existence of mtDNA G4s was supported by the long fluorescence decay time of the fluorescent ligand-G4 complex characterized with FLIM in live HeLa cells.

A benzoselenazolium-based hemicyanine dye, **SEMA-1**, is the most recently reported red-emitting ligand targeting mtDNA G4s.[167] The fluorescence titration experiments (λ_{ex}=615 nm, λ_{em}=660 nm) show that the ligand interacts with a number of G4s *in vitro*, in particular Pu22 showing better fluorescence enhancement compared to other nucleic acids. The K_D value of **SEMA-1** interacted with G4s was found in the range of 0.22–4.33 μM, indicating that the binding affinity of the ligand toward G4s was relatively strong. Moreover, live cell imaging and colocalization study of **SEMA-1** with MitoTracker Green in HeLa cells indicate that the ligand is mitochondria-specific (**Figure 8L**). The intracellular competition study with RHPS4 demonstrates that **SEMA-1** most probably interacts with mtDNA G4s in mitochondria.

4. Development of G4-selective ligands against bacteria and biofilm formation

Similar to human genome, the G4-forming DNA sequences identified in bacterial genomes are also found in various bacteria.[168] These G-rich sequences are also found enriched and conserved in regulatory regions of bacterial genomes.[169] It is thus believed that these G-rich sites may have important biofunctions in replication,[170] transcription[171] and translation[172]. Interestingly, compared to DNA, RNA G4s are not commonly present in bacteria. For example, there is only one RNA G4 site found in *Pseudomonas putida*.[43] In addition, a recent study reported that a DNA:RNA hybrid G4-structure was formed to mediate the transcription termination in bacterial cells.[173] The stabilization of G4s formed in the promoter region of bacterial genes with small molecules may

affect gene transcription.[174] The study on the regulatory role of bacterial G4s in virulence processes in the important microbial pathogens of human has been reviewed recently.[175]

TmPyP4 and a benzophenoxazine-based ligand **1**, shown in **Figure 9A**, are previously reported G4-ligands.[176, 177] These ligands are able to stabilize the G4s in the promoter region of the *nas* genes encoding the assimilatory nitrate/nitrite reductase system and then cause a reduction of gene transcription.[174] Moreover, an extended naphthalene di-imide ligand, **NDI-10**, was confirmed with biophysical assays in stabilizing the G4s formed from six selected G4-forming sequences of *E.coli* and *S. aureus*.[178] Interestingly, **NDI-10** exhibits different mechanisms in killing different types of bacteria: the bacteriostatic effect for Gram-positive bacteria and bactericidal effect for Gram-negative bacteria (**Figure 9B**). The different antibacterial activity profile may be due to the different prevalence of the putative DNA G4s in each group of bacterial strains. The ligand may thus influence different roles of the G4s in bacteria such as upregulating gene transcription in Gram-positive bacteria and repressing gene transcription in Gram-negatives. The MIC of **NDI-10** against *S. aureus* and *E. coli* was found to be 16 μM (**Table 1**).

Naphthalimide derivatives are reported as G4-DNA binding ligands and show potent antiparasitic activity.[179] An analogue ligand, **NI**, shown in **Figure 10 A**, exhibits antimicrobial activities against *Staphylococcus aureus* ATCC 29213 and *Enterococcus faecalis* ATCC 29212. It also shows inhibitory activity against Taq-polymerase and transcriptase.[180] **BRACO19**, its molecular structure shown in **Figure 3**, is a well-known potent G4-stabilizing agent. It has recent been discovered with strong ability to interact and stabilize the intracellular G4s of *Klebsiella pneumoniae* (*K. pneumoniae*).[181] In the study, six highly conserved G4s in the promoter region of five essential genes of *K. pneumoniae* were identified and investigated with **BRACO19** because these G4s play critical roles in nutrient transport and metabolism in bacteria. A strong association constant was observed for the interaction of **BRACO19** with G4-structure (K_a=5.92×10^{11} M^{-1}). The stabilization of these bacterial G4s with the ligand stops the primer extension process. Moreover, **BRACO19** downregulates the expression of the G4-harboring genes and also kills the bacterial cells. The IC_{50} of **BRACO19** against *K. puemoniae* (ATCC 700603) obtained was 10.77 μM.

Recently, the fluorescent G4-ligands derived from naphthoquinone-triazole derivatives have also been explored in antibacterial study.[182] This class of compounds at the concentration range of 4–128 μg/mL generally shows antibacterial activity. Two most active analogues, **5d** and **5e**, shown in **Figure 10 A**, exhibited the best antimicrobial ability. The lowest MIC against *Enterococcus hirae* (ATCC 10541) was 4 μg/mL. However, these two G4-ligands show less potency against *E. coli, S. aureus* and *P. aeruginosa* (**Table 1**).

Our group has also investigated some G4-DNA binding ligands developed recently in antibacterial study. The G4-ligands derived from the integration of 1-methylquinolinium and indole scaffolds[137, 183] were found showing certain degree of activity against a number of Gram-positive and Gram-negative bacterial strains.[184, 185] A screening from a small library of G4-ligands developed by our group shows that **c2** and **c9** (**Figure 10 A**) are the most potent compounds. The ligands inhibit effectively the growth of some selected strains including MRSA and VRE. The MICs obtained were in the range of 1–4 μg/mL by bactericidal mode.[184] Unexpectedly, from the mode of action assays, we found that **c2** disrupted the rate of GTP hydrolysis and dynamic polymerization of FtsZ. These cellular influences by the ligand may inhibit the bacterial cell division and cause bacterial cell death. More importantly, from the result of resistance generation experiments against *S. aureus* (ATCC 29213) after 17 passages, **c2** was not likely to induce drug resistance.

In addition to the antibacterial study with G4s as the drug target, research on bacterial biofilm formation and novel strategy for combating bacterial biofilm infections is also an emerging topic worldwide. Bacterial biofilm is one of the major factors that render bacteria being highly resistant to most clinical antibiotics. Bacterial biofilms are known contributed to persistent chronic infections and have been a serious global health concern because of their strong abilities to tolerate external stresses including most antibiotics and host immune systems. A number of recently published reviews have provided timely updates and also highlighted the current challenges and advances against bacterial biofilms.[186-190]

It was reported that a ubiquitous bacterial biofilm regulator (3′,5′-cyclic diguanylic acid (c-di-GMP)) was capable of forming G4s ten year ago.[191, 192] In addition, the extracellular DNA (eDNA) of the bacterial biofilm matrix contains G4s.[193] However, there are very few small-molecules or ligands reported in literature targeting these bacterial G4s to tackle bacterial biofilm infections. Some small-sized aromatic ligands (**Figure 10 B**) such as **acriflavine**,[191] **proflavine**,[191] and **diminaene**[194] are found able to interact with c-di-GMP and followed stabilizing the G4-structure of the tetrameric c-di-GMP (a higher-order tetrameric form) via π-stacking interactions. These G4-ligands upon binding to and stabilizing the G4 of c-di-GMP may inactive the biological function of c-di-GMP that plays a central role in the regulation of bacterial biofilm formation.[195, 196] Therefore, it is believed that to design potent and selective small ligands targeting c-di-GMP signalling may inhibit bacterial biofilm formation. This approach may be a new and effective antibiofilm strategy to tackle the antibiotic resistance due to bacterial biofilms.

Thiazole orange (**TO**) is reported capable of inducing c-di-GMP G4-structure formation and that facilitates the fluorescent detection of this important signaling molecule in bacteria.[197] Further structural modification from **TO**, ligand **A18** was synthesized as a new fluorescent probe for the

detection of c-di-GMP G4s at low concentration (500 nM).[198] Moreover, **A18** was able to distinguish c-di-GMP from other small nucleotides such as GMP and cGMP. However, all these reported c-di-GMP-targeting ligands discussed herein were only demonstrated as the selective fluorescent biosensors toward c-di-GMP G4s *in vitro* but none of them showed inhibitory activity against bacterial biofilm formation.[199] Until recently, a fluorescent ligand **5h** developed based on the integration of a thiazole and a guaiacol scaffold via a conjugated ethylene bridge was found to be an effective c-di-GMP G4-inducer and also a potent bacterial biofilm inhibitor against *P. aeruginosa* PAO1.[200] The cellular c-di-GMP-related biological functions in PAO1 was significantly interfered by the ligand. About 62% biofilm inhibitory activity was achieved with **5h** at 1.25 μM. Moreover, **5h** showed no any observable DNA intercalation effects, indicating that the ligand was highly selective toward c-di-GMP G4 in bacterial cells. These findings may support that targeting the higher-order c-di-GMP G4 in bacterial cells with potent G4-ligands, the strong c-di-GMP G4-inducers and stabilizers, could be a feasible strategy to develop novel and effective therapeutic methods against drug-resistant bacterial biofilms. It is expected that the target-specific and potent G4-ligand may induce the monomeric c-di-GMP to form the dysfunctional higher-order c-di-GMP G4s in live bacterial cells. The biofilm formation is thus repressed and the biofilm dispersion may be facilitated due to the local monomeric c-di-GMP concentration is reduced in bacteria.[201]

Table 1. The MIC values of some G4-ligands against the selected Gram-positive and Gram-negative bacteria. [a]

	Gram-positive bacteria		Gram-negative bacteria		
Ligand [b]	*S. aureus*	*E. faecalis*	*E. coli*	*K. pneumoniae*	*P. aeruginosa*
NDI-10	16 μM (LMG 8224)	4 μM (LMG 16216)	16 μM (LMG 8223)	> 128 μM (LMG 20218)	128 μM (LMG 6395)
NI	15.62 μM (ATCC 29213)	31.25 μM (ATCC 29212)	125 μM (ATCC 25922)	--	125 μM (ATCC 27853)
BRACO19	--	--	--	10.77 μM [c] (ATCC 700603)	--
5d	16 μM (ATCC 6538)	--	32 μM (ATCC 10536)	--	8 μM (ATCC 9027)
5e	16 μM (ATCC 6538)	--	32 μM (ATCC 10536)	--	16 μM (ATCC 9027)
c2	1 μg/mL (ATCC 25923)	4 μg/mL (ATCC 29212)	16 μg/mL (ATCC 25922)	> 64 μg/mL (BAA-2470) [d]	> 64 μg/mL (BAA-2108) [e]
c9	2 μg/mL (ATCC 25923)	4 μg/mL (ATCC 29212)	8 μg/mL (ATCC 25922)	> 64 μg/mL (BAA-2470) [d]	> 64 μg/mL (BAA-2108) [e]

[a] The information of bacterial strains is given in parenthesis. [b] The chemical structure of ligands was shown in **Figure 3** and **Figure 10A**. [c] The value given is IC_{50} determined by MTT-based growth inhibition assay. [d] The *K. pneumoniae* ATCC BAA-2470 stain expressing NDM-1 beta-lactamase. [e] *P. aeruginosa* ATCC BAA-2108 is a multidrug-resistant strain.

Table 2. The selected guanine-rich nucleic acid sequences with propensity to fold into G4-strucutres as the drug target for chemical biology and drug discovery study against human diseases.

	Source	Selected sequence (5' to 3')
1	Cytoplasmic membrane-associated DNA (cmDNA): 171-bp α-satellite repeat sequences[202]	*d*(*GG*AAT*GG*AAT*GG*AAT*GG*AAT) *d*(AT*GG*AAT*GG*AAT*GG*AAT*GG*A) *d*(T*GG*AAT*GG*AAT*GG*AAT*GG*AA) *d*(AAT*GG*AAT*GG*AAT*GG*AAT*GG*) *d*(*GG*TTA*GGG*TTA*GGG*TTA*GGG*) *d*(*GGG*TTA*GGG*TTA*GGG*TTA*GG*)
2	*Klebsiella pneumoniae* genomes: the promoter region[181]	*d*(*GGG*AGA*GGG*TT*GGGG*TGA*GGG*) *d*(*GGG*AGA*GGG*CC*GGGG*TGT*GGGG*) *d*(*GGGG*AGA*GGGG*AA*GGG*TGA*GGGG*) *d*(T*GGGGG*A*GGG*TTA*GGG*TGA*GGGG*) *d*(*GGG*AGA*GGG*TC*GGGG*TGA*GGGG*) *d*(*GGG*AGA*GGG*CC*GGGG*TGA*GGG*)
3	Transcriptome of *E. coli and P. aeruginosa*[203]	*hemL*: *r*(*GG*UCC*GG*UCUAUCA*GG*C*GGG*U) *bswR*: *r*(CU*GG*CCAU*GG*UCCUCCA*GG*UCCCCAU*GG*CC)
4	Cell division protein FtsZ (*E. coli* K-12) NCBI reference sequence: NC_000913.3	*r*(AAGUCAUC*GG*CGUC*GG*C*GG*C*GG*C*GG*C*GG*) *r*(*GGG*UAU*GGG*U*GG*U*GG*UACC*GG*UACA*GG*) *r*(*GGG*UUCU*GG*CGU*GG*CGAGC*GG*) *r*(*GG*UAGC*GG*UAUCACCAAA*GG*ACU*GGG*CGCU*GG*)

5. Summary and future perspectives

The discovery of G-quadruplex structures, in particular the one found in human telomeric non-coding G-rich repeats of DNA sequences ($(TTAGGG)_n$)[204], and afterward, characterized with *X*-ray crystal structure by Neidle and co-workers[205] and another one found in the coding G-rich DNA sequence located in the promoter region of the oncogene MYC by Hurley and co-workers,[176] has illuminated a unprecedented role of these special DNA secondary structures in biology (especially in cancer biology) over the past decades. Genome-wide analyses of a variety of species including human, chimpanzee, mouse, and rat promoters show that the enrichment of putative G4-forming sequences are located near transcription start sites.[9, 206] In addition, current findings anticipate substantial implications of DNA G4s as *cis*-regulatory factors on gene expression.[207] These observations sparked great interest on developing G4-targeting small molecules in drug discovery against cancers and other human diseases. Despite thousands of G4-ligands have been reported to date, only few including Quarfloxin (CX-3543) and Pidnarulex (CX-5461) enter human clinical trials. Quarfloxin has passed phase II trials as a candidate therapeutic agent against several tumors.[79] The results of Pidnarulex in phase I trial in patients with solid tumors also has just been

released.[208] It was found that the ligand was generally well tolerated with phototoxicity as the principal toxicity but exhibited modest antitumor activity when administered to unselected patients at a maximum dose.

Despite Quarfloxin and Pidnarulex have reached a new milestone, there is no G4-targeting drugs approved for clinical use at present. This indicates a big challenge ahead on realizing drug discovery with the use of G4s as the drug target. The challenge in developing small-molecule quadruplex therapeutics has been analyzed and discussed thoroughly in a recent review.[58] In the development of G4-targeting drugs, it may also encounter some critical challenges similarly to that of protein-targeting drugs. One of the key difficulties could be G4-binding compounds displaying low *in vivo* selectivity to G4s against the massive double-stranded DNA, proteins and other biomolecules in cells. The low target-specificity may result in unexpected side effects and cause the drug development process being halted. In addition, considering the current molecular design of G4-ligands as illustrated in **Figure 3**, the approach is still very limited and generally adopts the planar aromatic and/or heteroaromatic chromophore bearing positive charge(s) either on the aromatic unit or the side groups to enhance electrostatic interactions with the binding pocket of G4-structures. Increasing the molecular diversity and structural features in G4-ligand design may provide helps in identifying ligands with high selectivity against other nucleic acid structures and biomolecules *in vivo*.

Alternatively, to develop G4-ligands targeting RNA G4s with high affinity and preferentially localized in cytoplasm may able to avoid or reduce the off-target interactions with the massive nuclear DNA in the nucleus; however, the spatial structural information such as high-resolution NMR or crystal structure for the critical drug target of mRNA G4s is currently lacking. This largely increases the difficulty for molecular chemists in designing ligands targeting mRNA G4s with high selectivity. For example, the crystal structure of RAS mRNA G4s such as KRAS, NRAS and HRAS are not available at present. Nonetheless, designing mRNA G4-selective ligands that are more favourably localized in cytoplasm than nucleus could be an attractive alternative for the "undruggable" protein targets such as BCL, RAS and MYC in cancer therapy.[209] Another challenge for ligand-RNA G4 interaction is that the mRNA concentration in cytoplasm is very low.

Apart from targeting RNA G4s, cytoplasmic membrane-associated DNA (cmDNA) could be a G4-target. cmDNA is a species of DNA attaching to the plasma membrane and originates in the genome and is present in intact cells. The analysis of cmDNA by deep sequencing reveals that the 171-bp α-satellite repeat sequences are highly enriched in cmDNA and are also found G-rich.[202] Some of these sequences with potential to fold into G4-structures are selected and listed in **Table 2**. cmDNA is currently studied in the context of apoptosis; however, there is no investigation reported on its G4 property and biofunctions associated with their G4-structures. The G4s of

cmDNA could be an interesting target to be further explored for their unknown roles, if any, in biology in the future.

The putative G4-forming sequences of bacteria are also identified as a potential drug target for drug discovery against antibiotic resistance. It is known that bacteria are residents in human tumors but the tumor microbiome has not been well-characterized. A recent study reported that each tumor type had a distinct microbiome composition and, interestingly, breast cancer was found showing a particularly rich and diverse microbiome.[210] At present, it is still unclear whether bacteria play a causal role in tumorigenesis. Nonetheless, G4s can be applied as a potential drug target for both anticancer and antibacterial. Whether or not these common G4-targets found in both cancer cells and bacterial cells could possibly offer a synergistic effect for anticancer therapy is of interest to further explore.

Some G4-forming sequences are also identified in *K. pneumoniae* and could be potentially utilized as a drug target for the development antibacterial agents with a new mechanism of action different from beta-lactam antibiotics that inhibit bacterial cell wall synthesis (**Table 2**). Interestingly, these sequences are conserved in the gene promoter region of *K. pneumoniae* genomes.[181] Therefore, drugs targeting these G4-forming sequences may possibly reduce or avoid drug-resistance due to gene mutation, because the conserved genes in bacteria may not be easily endured mutation. In addition to bacterial DNA G4s, bacterial RNA G4 sites in the transcriptome of *E. coli* and *P. aeruginosa* were also identified.[203] For example, two RNA G4 sites in bacteria (**Table 2**: *hemL* and *bswR*) were verified to show regulatory functions. These RNA G4 sites may be utilized as a drug target because the bacterial genes carrying these sites are found implicated in virulence, gene regulation, cell envelope synthesis, and metabolism.

Furthermore, a critically important bacterial cell division protein, filamenting temperature-sensitive mutant Z (FtsZ), is recognized as a vital drug target in new antibiotic discovery against antibacterial resistance. It is because FtsZ is conserved among most bacterial strains. Despite researchers have devoted great efforts to develop numerous inhibitors against this bacterial protein, FtsZ is still a very challenging target for the discovery of new antibiotics. To further address the current bottleneck, exploring better alternative strategies may be able to provide a breakthrough. The mRNA sequence for encoding FtsZ is also G-rich. The full-length FtsZ mRNA sequence contains many putative G4-forming sites. Some of these sites are selected and listed in **Table 2**. Nonetheless, the study on these mRNA G4s has not yet been reported. It is probably due to the structural information of FtsZ mRNA G4s is currently lacking for ligand design and that significantly hinders the R&D progress on this direction. Because the field of G-quadruplex is very diverse in terms of structures and sequences that without knowing the sequence exactly, it becomes extremely difficult to design sequence specific drugs. Apart from obtaining *X*-ray crystal structures

for G4-targets, the use of advanced computational tools such as molecular docking and simulation, artificial intelligence and/or machine learning for pushing high-throughput drug design, and also the high-resolution NMR spectroscopy and advanced microscopy techniques including high throughput microscopy and cryo-TEM for validation of these G4-drugs may provide useful information and help move forward in the track to realize G4-drug discovery, particularly the anticancer and antibacterial drugs, against life-threatening diseases.

Acknowledgements

The work was substantially supported by the grant from the Research Grants Council of the Hong Kong Special Administrative Region, China (RGC Project No. 15300522); Health and Medical Research Fund (HMRF), Hong Kong SAR (Project No. 19200231); The Hong Kong Polytechnic University, PolyU Startup Fund (P0035712 and P0043754) and PolyU SZRI Fund (P0039278).

Competing interests

The authors declare no competing interests.

Reference

1. S. B. Zimmerman, G. H. Cohen and D. R. Davies, *Journal of molecular biology*, 1975, **92**, 181-192.
2. F. Howard, J. Frazier and H. T. Miles, *Biopolymers: Original Research on Biomolecules*, 1977, **16**, 791-809.
3. S. Burge, G. N. Parkinson, P. Hazel, A. K. Todd and S. Neidle, *Nucleic acids research*, 2006, **34**, 5402-5415.
4. J. L. Huppert, *Chemical Society Reviews*, 2008, **37**, 1375-1384.
5. H. L. Lightfoot, T. Hagen, N. J. Tatum and J. Hall, *FEBS letters*, 2019, **593**, 2083-2102.
6. M. Kaushik, S. Kaushik, A. Bansal, S. Saxena and S. Kukreti, *Current Molecular Medicine*, 2011, **11**, 744-769.
7. X. Yang, J. Cheema, Y. Zhang, H. Deng, S. Duncan, M. I. Umar, J. Zhao, Q. Liu, X. Cao and C. K. Kwok, *Genome biology*, 2020, **21**, 1-23.
8. V. S. Chambers, G. Marsico, J. M. Boutell, M. Di Antonio, G. P. Smith and S. Balasubramanian, *Nature biotechnology*, 2015, **33**, 877-881.
9. A. Vannutelli, S. Belhamiti, J.-M. Garant, A. Ouangraoua and J.-P. Perreault, *NAR genomics and bioinformatics*, 2020, **2**, lqaa035.
10. P. H. Wanrooij, J. P. Uhler, T. Simonsson, M. Falkenberg and C. M. Gustafsson, *Proceedings of the National Academy of Sciences*, 2010, **107**, 16072-16077.
11. M. Falabella, R. J. Fernandez, F. B. Johnson and B. A. Kaufman, *Current medicinal chemistry*, 2019, **26**, 2918-2932.
12. K. Agaronyan, Y. I. Morozov, M. Anikin and D. Temiakov, *Science*, 2015, **347**, 548-551.
13. T. Kamura, Y. Katsuda, Y. Kitamura and T. Ihara, *Biochemical and biophysical research communications*, 2020, **526**, 261-266.
14. P. Kharel, G. Becker, V. Tsvetkov and P. Ivanov, *Nucleic acids research*, 2020, **48**, 12534-12555.
15. D. Varshney, J. Spiegel, K. Zyner, D. Tannahill and S. Balasubramanian, *Nature Reviews Molecular Cell Biology*, 2020, **21**, 459-474.
16. J. Spiegel, S. Adhikari and S. Balasubramanian, *Trends in Chemistry*, 2020, **2**, 123-136.
17. T. Tian, Y.-Q. Chen, S.-R. Wang and X. Zhou, *Chem*, 2018, **4**, 1314-1344.

18. R. Hänsel-Hertsch, M. Di Antonio and S. Balasubramanian, *Nature reviews Molecular cell biology*, 2017, **18**, 279-284.
19. P. Sengupta, S. Chattopadhyay and S. Chatterjee, *Drug Discov. Today*, 2017, **22**, 1165-1186.
20. M. M. Fay, S. M. Lyons and P. Ivanov, *Journal of molecular biology*, 2017, **429**, 2127-2147.
21. S. Rouleau, R. Jodoin, J.-M. Garant and J.-P. Perreault, *Catalytically active nucleic acids*, 2017, 1-20.
22. N. Dolinnaya, A. Ogloblina and M. Yakubovskaya, *Biochemistry (Moscow)*, 2016, **81**, 1602-1649.
23. D. Rhodes and H. J. Lipps, *Nucleic acids research*, 2015, **43**, 8627-8637.
24. N. Saini, Y. Zhang, K. Usdin and K. S. Lobachev, *Biochimie*, 2013, **95**, 117-123.
25. M. L. Bochman, K. Paeschke and V. A. Zakian, *Nature Reviews Genetics*, 2012, **13**, 770-780.
26. G. W. Collie and G. N. Parkinson, *Chemical Society Reviews*, 2011, **40**, 5867-5892.
27. K.-I. Oh, J. Kim, C.-J. Park and J.-H. Lee, *International Journal of Molecular Sciences*, 2020, **21**, 2673.
28. M. Adrian, B. Heddi and A. T. Phan, *Methods*, 2012, **57**, 11-24.
29. S. M. Haider, S. Neidle and G. N. Parkinson, *Biochimie*, 2011, **93**, 1239-1251.
30. G. N. Parkinson and G. W. Collie, in *G-Quadruplex Nucleic Acids*, Springer, 2019, pp. 131-155.
31. A. E. Engelhart, *Nature Chemical Biology*, 2017, **13**, 1140-1141.
32. N. Campbell, G. W. Collie and S. Neidle, *Current Protocols in Nucleic Acid Chemistry*, 2012, **50**, 17.16. 11-17.16. 22.
33. H. Xi, M. Juhas and Y. Zhang, *Biosensors and Bioelectronics*, 2020, **167**, 112494.
34. S. Manna and S. G. Srivatsan, *RSC advances*, 2018, **8**, 25673-25694.
35. A. C. Bhasikuttan and J. Mohanty, *Chemical Communications*, 2015, **51**, 7581-7597.
36. J. Ren, T. Wang, E. Wang and J. Wang, *Analyst*, 2015, **140**, 2556-2572.
37. Y. Tang, B. Ge, D. Sen and H.-Z. Yu, *Chemical Society Reviews*, 2014, **43**, 518-529.
38. B. R. Vummidi, J. Alzeer and N. W. Luedtke, *ChemBioChem*, 2013, **14**, 540-558.
39. G. Biffi, M. Di Antonio, D. Tannahill and S. Balasubramanian, *Nature chemistry*, 2014, **6**, 75-80.
40. G. Biffi, D. Tannahill, J. McCafferty and S. Balasubramanian, *Nature chemistry*, 2013, **5**, 182-186.
41. Y. Xu and M. Komiyama, *ChemBioChem*, 2013, **14**, 927-928.
42. A. Henderson, Y. Wu, Y. C. Huang, E. A. Chavez, J. Platt, F. B. Johnson, R. M. Brosh, D. Sen and P. M. Lansdorp, *Nucleic acids research*, 2013, **42**, 860-869.
43. J. U. Guo and D. P. Bartel, *Science*, 2016, **353**, aaf5371.
44. H. J. Lipps and D. Rhodes, *Trends in cell biology*, 2009, **19**, 414-422.
45. C. Zhang, H.-h. Liu, K.-w. Zheng, Y.-h. Hao and Z. Tan, *Nucleic acids research*, 2013, **41**, 7144-7152.
46. S. Y. Yang, P. Lejault, S. Chevrier, R. Boidot, A. G. Robertson, J. M. Wong and D. Monchaud, *Nature communications*, 2018, **9**, 1-11.
47. E. H. Blackburn and J. G. Gall, *Journal of molecular biology*, 1978, **120**, 33-53.
48. D. R. Corey, *Chemistry & biology*, 2009, **16**, 1219-1223.
49. C. W. Greider and E. H. Blackburn, *cell*, 1985, **43**, 405-413.
50. E. Varela and M. Blasco, *Oncogene*, 2010, **29**, 1561-1565.
51. L.-Y. Zhai, J.-F. Liu, J.-J. Zhao, A.-M. Su, X.-G. Xi and X.-M. Hou, *Journal of Medicinal Chemistry*, 2022, **65**, 10161-10182.
52. P. Kharel, S. Balaratnam, N. Beals and S. Basu, *Wiley Interdisciplinary Reviews: RNA*, 2020, **11**, e1568.
53. E. Ruggiero and S. N. Richter, in *Annual reports in medicinal chemistry*, Elsevier, 2020, vol. 54, pp. 101-131.
54. J. Plavec, in *Annual Reports in Medicinal Chemistry*, Elsevier, 2020, vol. 54, pp. 441-483.
55. S. Asamitsu, M. Takeuchi, S. Ikenoshita, Y. Imai, H. Kashiwagi and N. Shioda, *International Journal of Molecular Sciences*, 2019, **20**, 2884.
56. A. Cammas and S. Millevoi, *Nucleic acids research*, 2017, **45**, 1584-1595.
57. V. Sanchez-Martin, C. Lopez-Pujante, M. Soriano-Rodriguez and J. A. Garcia-Salcedo, *International Journal of Molecular Sciences*, 2020, **21**, 8900.
58. S. Neidle, in *Annual Reports in Medicinal Chemistry*, Elsevier, 2020, vol. 54, pp. 517-546.

59. H. Seimiya, *Cancer Science*, 2020, **111**, 3089-3099.
60. C. Nakanishi and H. Seimiya, *Biochemical and biophysical research communications*, 2020, **531**, 45-50.
61. J. Carvalho, J.-L. Mergny, G. F. Salgado, J. A. Queiroz and C. Cruz, *Trends in molecular medicine*, 2020, **26**, 848-861.
62. G. Miglietta, M. Russo and G. Capranico, *Nucleic Acids Research*, 2020, **48**, 11942-11957.
63. W. Wang, S. Hu, Y. Gu, Y. Yan, D. B. Stovall, D. Li and G. Sui, *Biochimica et Biophysica Acta (BBA)-Reviews on Cancer*, 2020, **1874**, 188410.
64. T. M. Bryan, *Molecules*, 2020, **25**, 3686.
65. L. E. Xodo, in *Annual Reports in Medicinal Chemistry*, Elsevier, 2020, vol. 54, pp. 325-359.
66. M. Singh, R. Gupta, L. Comez, A. Paciaroni, R. Rani and V. Kumar, *Drug Discovery Today*, 2022.
67. I. Alessandrini, M. Recagni, N. Zaffaroni and M. Folini, *International journal of molecular sciences*, 2021, **22**, 5947.
68. E. Mendes, I. M. Aljnadi, B. Bahls, B. L. Victor and A. Paulo, *Pharmaceuticals*, 2022, **15**, 300.
69. G. N. Parkinson and H. Berman, *Bioorganic & Medicinal Chemistry*, 2022, 116887.
70. E. Puig Lombardi and A. Londoño-Vallejo, *Nucleic acids research*, 2020, **48**, 1-15.
71. F. Ilaria, P. Valentina, N. R. Sara and D. Filippo, *International Journal of Biological Macromolecules*, 2022.
72. R. C. Monsen, S. Chakravarthy, W. L. Dean, J. B. Chaires and J. O. Trent, *Nucleic acids research*, 2021, **49**, 1749-1768.
73. N. Smargiasso, F. Rosu, W. Hsia, P. Colson, E. S. Baker, M. T. Bowers, E. De Pauw and V. Gabelica, *Journal of the American Chemical Society*, 2008, **130**, 10208-10216.
74. S. Balasubramanian, L. H. Hurley and S. Neidle, *Nature reviews Drug discovery*, 2011, **10**, 261-275.
75. N. Maizels, *EMBO reports*, 2015, **16**, 910-922.
76. N. Kosiol, S. Juranek, P. Brossart, A. Heine and K. Paeschke, *Molecular Cancer*, 2021, **20**, 1-18.
77. G. Biffi, D. Tannahill, J. Miller, W. J. Howat and S. Balasubramanian, *PloS one*, 2014, **9**, e102711.
78. C. Li, H. Wang, Z. Yin, P. Fang, R. Xiao, Y. Xiang, W. Wang, Q. Li, B. Huang and J. Huang, *Genome research*, 2021, **31**, 1546-1560.
79. V. Sanchez-Martin, M. Soriano and J. A. Garcia-Salcedo, *Cancers*, 2021, **13**, 3156.
80. A. Awadasseid, X. Ma, Y. Wu and W. Zhang, *Biomedicine & Pharmacotherapy*, 2021, **139**, 111550.
81. W. Long, B.-X. Zheng, Y. Li, X.-H. Huang, D.-M. Lin, C.-C. Chen, J.-Q. Hou, T.-M. Ou, W.-L. Wong and K. Zhang, *Nucleic acids research*, 2022, **50**, 1829-1848.
82. H.-J. Sullivan, C. Readmond, C. Radicella, V. Persad, T. J. Fasano and C. Wu, *ACS omega*, 2018, **3**, 14788-14806.
83. N. Sun, C. Wang, M.-H. Xu, Y.-J. Lu, Y.-Y. Zheng, Y. Yan, X.-L. Guo, J. Hou, K. Zhang and L. G. Luyt, *Sensors and Actuators B: Chemical*, 2017, **250**, 543-551.
84. Y.-J. Lu, Q. Deng, J.-Q. Hou, D.-P. Hu, Z.-Y. Wang, K. Zhang, L. G. Luyt, W.-L. Wong and C.-F. Chow, *ACS Chemical Biology*, 2016, **11**, 1019-1029.
85. W. J. Chung, B. Heddi, M. Tera, K. Iida, K. Nagasawa and A. T. Phan, *Journal of the American Chemical Society*, 2013, **135**, 13495-13501.
86. T. A. Brooks and L. H. Hurley, *Nature Reviews Cancer*, 2009, **9**, 849-861.
87. D. Hanahan and R. A. Weinberg, *cell*, 2000, **100**, 57-70.
88. G. Miglietta, J. Marinello, M. Russo and G. Capranico, *Molecular Cancer*, 2022, **21**, 1-15.
89. S. Zhang, H. Sun, L. Wang, Y. Liu, H. Chen, Q. Li, A. Guan, M. Liu and Y. Tang, *Nucleic acids research*, 2018, **46**, 7522-7532.
90. M. Di Antonio, A. Ponjavic, A. Radzevičius, R. T. Ranasinghe, M. Catalano, X. Zhang, J. Shen, L.-M. Needham, S. F. Lee and D. Klenerman, *Nature chemistry*, 2020, **12**, 832-837.
91. L. Y. Liu, W. Liu, K. N. Wang, B. C. Zhu, X. Y. Xia, L. N. Ji and Z. W. Mao, *Angewandte Chemie*, 2020, **132**, 9806-9813.
92. P. A. Summers, B. W. Lewis, J. Gonzalez-Garcia, R. M. Porreca, A. H. Lim, P. Cadinu, N. Martin-Pintado, D. J. Mann, J. B. Edel and J. B. Vannier, *Nature communications*, 2021, **12**, 1-11.

93. Q. Zhai, C. Gao, J. Ding, Y. Zhang, B. Islam, W. Lan, H. Hou, H. Deng, J. Li and Z. Hu, *Nucleic acids research*, 2019, **47**, 2190-2204.
94. F. Raguseo, S. Chowdhury, A. Minard and M. Di Antonio, *Chemical Communications*, 2020, **56**, 1317-1324.
95. J.-H. Yuan, W. Shao, S.-B. Chen, Z.-S. Huang and J.-H. Tan, *Biochemical and Biophysical Research Communications*, 2020, **531**, 18-24.
96. L. Zhao, F. Ahmed, Y. Zeng, W. Xu and H. Xiong, *ACS sensors*, 2022.
97. A. Pandith, R. G. Siddappa and Y. J. Seo, *Journal of Photochemistry and Photobiology C: Photochemistry Reviews*, 2019, **40**, 81-116.
98. V. Dhamodharan and P. Pradeepkumar, *ACS Chemical Biology*, 2019, **14**, 2102-2114.
99. P. Chilka, N. Desai and B. Datta, *Molecules*, 2019, **24**, 752.
100. K. TaeáKim and B. HyeanáKim, *Chemical Communications*, 2016, **52**, 12757-12760.
101. Z.-S. Wu, P. Hu, H. Zhou, G. Shen and R. Yu, *Biomaterials*, 2010, **31**, 1918-1924.
102. M. I. Umar, D. Ji, C.-Y. Chan and C. K. Kwok, *Molecules*, 2019, **24**, 2416.
103. R. V. Brown, F. L. Danford, V. Gokhale, L. H. Hurley and T. A. Brooks, *Journal of Biological Chemistry*, 2011, **286**, 41018-41027.
104. H.-S. Huang, I.-B. Chen, K.-F. Huang, W.-C. Lu, F.-Y. Shieh, Y.-Y. Huang, F.-C. Huang and J.-J. Lin, *Chemical and pharmaceutical bulletin*, 2007, **55**, 284-292.
105. E. Izbicka, R. T. Wheelhouse, E. Raymond, K. K. Davidson, R. A. Lawrence, D. Sun, B. E. Windle, L. H. Hurley and D. D. Von Hoff, *Cancer research*, 1999, **59**, 639-644.
106. M. Franceschin, L. Rossetti, A. D'Ambrosio, S. Schirripa, A. Bianco, G. Ortaggi, M. Savino, C. Schultes and S. Neidle, *Bioorganic & Medicinal Chemistry Letters*, 2006, **16**, 1707-1711.
107. J. Dickerhoff, N. Brundridge, S. A. McLuckey and D. Yang, *Journal of Medicinal Chemistry*, 2021, **64**, 16205-16212.
108. S. M. Gowan, J. R. Harrison, L. Patterson, M. Valenti, M. A. Read, S. Neidle and L. R. Kelland, *Molecular pharmacology*, 2002, **61**, 1154-1162.
109. G. N. Parkinson, R. Ghosh and S. Neidle, *Biochemistry*, 2007, **46**, 2390-2397.
110. A. De Cian, E. DeLemos, J.-L. Mergny, M.-P. Teulade-Fichou and D. Monchaud, *Journal of the American Chemical Society*, 2007, **129**, 1856-1857.
111. R. Rodriguez, S. Müller, J. A. Yeoman, C. Trentesaux, J.-F. Riou and S. Balasubramanian, *Journal of the American Chemical Society*, 2008, **130**, 15758-15759.
112. L.-Y. Liu, T.-Z. Ma, Y.-L. Zeng, W. Liu and Z.-W. Mao, *Journal of the American Chemical Society*, 2022, **144**, 11878-11887.
113. J. Mohanty, N. Barooah, V. Dhamodharan, S. Harikrishna, P. Pradeepkumar and A. C. Bhasikuttan, *Journal of the American Chemical Society*, 2013, **135**, 367-376.
114. L. Xu, X. Shen, S. Hong, J. Wang, Y. Zhang, H. Wang, J. Zhang and R. Pei, *Chemical Communications*, 2015, **51**, 8165-8168.
115. F. Y. Khusbu, X. Zhou, H. Chen, C. Ma and K. Wang, *TrAC Trends in Analytical Chemistry*, 2018, **109**, 1-18.
116. Y. Zhu, J. Hou, X.-H. Huang, D.-X. Zhong, W. Long, W. Liu, Y.-J. Lu, K. Zhang and W.-L. Wong, *Journal of Luminescence*, 2020, **226**, 117488.
117. N. Sun, D. Li, J. Hou, W. Long, Q. Guo, Y. Lu, K. Zhang, W. Yuan and W. L. Wong, *Chemical Biology & Drug Design*, 2019, **93**, 979-985.
118. Y.-J. Lu, D.-P. Hu, K. Zhang, W.-L. Wong and C.-F. Chow, *Biosensors and Bioelectronics*, 2016, **81**, 373-381.
119. J. Jin, J. Hou, W. Long, X. Zhang, Y.-J. Lu, D. Li, K. Zhang and W.-L. Wong, *Bioorganic Chemistry*, 2020, **99**, 103821.
120. D. Li, W. Long, J. Hou, Q. Deng, Q. Guo, W.-L. Wong, Y.-J. Lu and K. Zhang, *Journal of Luminescence*, 2019, **205**, 367-373.
121. D. Li, J.-Q. Hou, W. Long, Y.-J. Lu, W.-L. Wong and K. Zhang, *RSC advances*, 2018, **8**, 20222-20227.
122. W. Long, Y.-J. Lu, K. Zhang, X.-H. Huang, J.-Q. Hou, S.-Y. Cai, Y. Li, X. Du, L. G. Luyt and W.-L. Wong, *Dyes and Pigments*, 2018, **159**, 449-456.

123. Y.-J. Lu, S.-C. Yan, F.-Y. Chan, L. Zou, W.-H. Chung, W.-L. Wong, B. Qiu, N. Sun, P.-H. Chan and Z.-S. Huang, *Chemical Communications*, 2011, **47**, 4971-4973.
124. Y.-J. Lu, Z.-Y. Wang, D.-P. Hu, Q. Deng, B.-H. Huang, Y.-X. Fang, K. Zhang, W.-L. Wong and C.-F. Chow, *Dyes and Pigments*, 2015, **122**, 94-102.
125. B.-X. Zheng, M.-T. She, W. Long, Y.-Y. Xu, Y.-H. Zhang, X.-H. Huang, W. Liu, J.-Q. Hou, W.-L. Wong and Y.-J. Lu, *Chemical Communications*, 2020, **56**, 15016-15019.
126. B.-X. Zheng, W. Long, Y.-H. Zhang, X.-H. Huang, C.-C. Chen, D.-X. Zhong, M.-T. She, Z.-X. Chen, D.-P. Cai and Y.-J. Lu, *Sensors and Actuators B: Chemical*, 2020, **314**, 128075.
127. W. Long, B.-X. Zheng, X.-H. Huang, M.-T. She, A.-L. Liu, K. Zhang, W.-L. Wong and Y.-J. Lu, *Journal of Medicinal Chemistry*, 2021, **64**, 2125-2138.
128. M.-T. She, J.-W. Yang, B.-X. Zheng, W. Long, X.-H. Huang, J.-R. Luo, Z.-X. Chen, A.-L. Liu, D.-P. Cai and W.-L. Wong, *Chemical Engineering Journal*, 2022, 136947.
129. W. J. Chung, B. Heddi, F. Hamon, M. P. Teulade‐Fichou and A. T. Phan, *Angewandte Chemie International Edition*, 2014, **53**, 999-1002.
130. Y. Katsuda, S.-i. Sato, M. Inoue, H. Tsugawa, T. Kamura, T. Kida, R. Matsumoto, S. Asamitsu, N. Shioda and S. Shiroto, *Nucleic acids research*, 2022, **50**, 8143-8153.
131. L. Dumas, P. Herviou, E. Dassi, A. Cammas and S. Millevoi, *Trends in Biochemical Sciences*, 2021, **46**, 270-283.
132. P. Herviou, M. Le Bras, L. Dumas, C. Hieblot, J. Gilhodes, G. Cioci, J.-P. Hugnot, A. Ameadan, F. Guillonneau and E. Dassi, *Nature communications*, 2020, **11**, 1-17.
133. A. L. Wolfe, K. Singh, Y. Zhong, P. Drewe, V. K. Rajasekhar, V. R. Sanghvi, K. J. Mavrakis, M. Jiang, J. E. Roderick and J. Van der Meulen, *Nature*, 2014, **513**, 65-70.
134. A. J. Zheng, A. Thermou, P. G. Gallardo, L. Malbert-Colas, C. Daskalogianni, N. Vaudiau, P. Brohagen, A. Granzhan, M. Blondel and M.-P. Teulade-Fichou, *Life science alliance*, 2022, **5**.
135. M. T. Banco and A. R. Ferré-D'Amaré, *Rna*, 2021, **27**, 390-402.
136. Y.-J. Lu, Q. Deng, D.-P. Hu, Z.-Y. Wang, B.-H. Huang, Z.-Y. Du, Y.-X. Fang, W.-L. Wong, K. Zhang and C.-F. Chow, *Chemical Communications*, 2015, **51**, 15241-15244.
137. C. Wang, Y.-J. Lu, S.-Y. Cai, W. Long, Y.-Y. Zheng, J.-W. Lin, Y. Yan, X.-H. Huang, W.-L. Wong and K. Zhang, *Sensors and Actuators B: Chemical*, 2018, **262**, 386-394.
138. B. Shirinfar, H. Seema and N. Ahmed, *Organic & Biomolecular Chemistry*, 2018, **16**, 164-168.
139. Y. Suseela, N. Narayanaswamy, S. Pratihar and T. Govindaraju, *Chemical Society Reviews*, 2018, **47**, 1098-1131.
140. Q. Li and Y.-T. Chang, *Nature Protocols*, 2006, **1**, 2922-2932.
141. L. Wang, Q. Xia, R. Liu and J. Qu, *Sensors and Actuators B: Chemical*, 2018, **273**, 935-943.
142. S. Xu, Q. Li, J. Xiang, Q. Yang, H. Sun, A. Guan, L. Wang, Y. Liu, L. Yu and Y. Shi, *Nucleic acids research*, 2015, **43**, 9575-9586.
143. A. l. Laguerre, K. Hukezalie, P. Winckler, F. Katranji, G. t. Chanteloup, M. Pirrotta, J.-M. Perrier-Cornet, J. M. Wong and D. Monchaud, *Journal of the American Chemical Society*, 2015, **137**, 8521-8525.
144. X. C. Chen, S. B. Chen, J. Dai, J. H. Yuan, T. M. Ou, Z. S. Huang and J. H. Tan, *Angewandte Chemie*, 2018, **130**, 4792-4796.
145. Z.-Y. Yu, W.-H. Luo, X.-C. Chen, S.-B. Chen, Z.-S. Huang and J.-H. Tan, *Sensors and Actuators B: Chemical*, 2020, **324**, 128770.
146. L. Yu, P. Verwilst, I. Shim, Y.-Q. Zhao, Y. Zhou and J. S. Kim, *CCS Chemistry*, 2021, **3**, 2725-2739.
147. Y. Zhang, K. El Omari, R. Duman, S. Liu, S. Haider, A. Wagner, G. N. Parkinson and D. Wei, *Nucleic acids research*, 2020, **48**, 9886-9898.
148. D. W. Dong, F. Pereira, S. P. Barrett, J. E. Kolesar, K. Cao, J. Damas, L. A. Yatsunyk, F. B. Johnson and B. A. Kaufman, *BMC genomics*, 2014, **15**, 1-15.
149. S. Mishra, S. Kota, R. Chaudhary and H. Misra, *Critical Reviews in Biochemistry and Molecular Biology*, 2021, **56**, 482-499.
150. M. M. Naeem, R. Maheshan, S. R. Costford, A. Wahedi, M. Trajkovski, J. Plavec, L. A. Yatsunyk, G. L. Ciesielski, B. A. Kaufman and N. Sondheimer, *Human Molecular Genetics*, 2019, **28**, 3163-3174.

151. T. J. Butler, K. N. Estep, J. A. Sommers, R. W. Maul, A. Z. Moore, S. Bandinelli, F. Cucca, M. A. Tuke, A. R. Wood and S. K. Bharti, *Human molecular genetics*, 2020, **29**, 1292-1309.
152. R.-Q. Yao, C. Ren, Z.-F. Xia and Y.-M. Yao, *Autophagy*, 2021, **17**, 385-401.
153. A. A. Khan, K. S. Allemailem, A. Almatroudi, S. A. Almatroodi, M. A. Alsahli and A. H. Rahmani, *Journal of Drug Delivery Science and Technology*, 2021, **61**, 102315.
154. Y. Wang, N. Chen, Z. Pan, Z. Ye, J. Yuan, Y. Zeng, W. Long, W. Bian, X. Li and Y.-J. Lu, *Chemical Engineering Journal*, 2022, **441**, 135977.
155. X. Guo, H. Chen, Y. Liu, D. Yang, Q. Li, H. Du, M. Liu, Y. Tang and H. Sun, *Journal of Materials Chemistry B*, 2022, **10**, 430-437.
156. H. Chen, H. Sun, S. Zhang, W. Yan, Q. Li, A. Guan, J. Xiang, M. Liu and Y. Tang, *Chemical Communications*, 2019, **55**, 5060-5063.
157. L.-L. Li, H.-R. Xu, K. Li, Q. Yang, S.-L. Pan and X.-Q. Yu, *Sensors and Actuators B: Chemical*, 2019, **286**, 575-582.
158. S. Liu, L. Bu, Y. Zhang, J. Yan, L. Li, G. Li, Z. Song and J. Huang, *Analytical Chemistry*, 2021, **93**, 5267-5276.
159. P. Hanczyc, P. Rajchel-Mieldzioć, B. Feng and P. Fita, *The Journal of Physical Chemistry Letters*, 2021, **12**, 5436-5442.
160. Z. Xu and L. Xu, *Chemical Communications*, 2016, **52**, 1094-1119.
161. X.-C. Chen, G.-X. Tang, W.-H. Luo, W. Shao, J. Dai, S.-T. Zeng, Z.-S. Huang, S.-B. Chen and J.-H. Tan, *Journal of the American Chemical Society*, 2021, **143**, 20779-20791.
162. X. Wang, B.-Y. Yu, J.-H. Lin, Y. Yan and M.-H. Hu, *Sensors and Actuators B: Chemical*, 2021, **330**, 129391.
163. M.-H. Hu, *Analytica Chimica Acta*, 2021, **1169**, 338600.
164. Y. V. Suseela, P. Satha and T. Govindaraju, *Analysis & Sensing*, 2021, **1**, 180-187.
165. K.-K. Yu, K. Li, H.-Z. He, Y.-H. Liu, J.-K. Bao and X.-Q. Yu, *Sensors and Actuators B: Chemical*, 2020, **321**, 128479.
166. W.-C. Huang, T.-Y. Tseng, Y.-T. Chen, C.-C. Chang, Z.-F. Wang, C.-L. Wang, T.-N. Hsu, P.-T. Li, C.-T. Chen and J.-J. Lin, *Nucleic acids research*, 2015, **43**, 10102-10113.
167. Z.-C. Li, T.-Y. Wu, S.-T. Zeng, L. Fang, J.-X. Mao, S.-B. Chen, Z.-S. Huang, X.-C. Chen and J.-H. Tan, *Bioorganic & Medicinal Chemistry Letters*, 2022, 128801.
168. P. Yadav, N. Kim, M. Kumari, S. Verma, T. K. Sharma, V. Yadav and A. Kumar, *Journal of Bacteriology*, 2021, **203**, e00577-00520.
169. S. K. Mishra, N. Jain, U. Shankar, A. Tawani, T. K. Sharma and A. Kumar, *Scientific reports*, 2019, **9**, 1-13.
170. R. Perrone, E. Lavezzo, E. Riello, R. Manganelli, G. Palù, S. Toppo, R. Provvedi and S. N. Richter, *Scientific reports*, 2017, **7**, 1-11.
171. N. Beaume, R. Pathak, V. K. Yadav, S. Kota, H. S. Misra, H. K. Gautam and S. Chowdhury, *Nucleic acids research*, 2013, **41**, 76-89.
172. I. T. Holder and J. S. Hartig, *Chemistry & biology*, 2014, **21**, 1511-1521.
173. R. y. Wu, K. w. Zheng, J. y. Zhang, Y. h. Hao and Z. Tan, *Angewandte Chemie International Edition*, 2015, **54**, 2447-2451.
174. Z. A. Waller, B. J. Pinchbeck, B. S. Buguth, T. G. Meadows, D. J. Richardson and A. J. Gates, *Chemical Communications*, 2016, **52**, 13511-13514.
175. L. M. Harris and C. J. Merrick, *PLoS pathogens*, 2015, **11**, e1004562.
176. A. Siddiqui-Jain, C. L. Grand, D. J. Bearss and L. H. Hurley, *Proceedings of the National Academy of Sciences*, 2002, **99**, 11593-11598.
177. K. I. McLuckie, Z. A. Waller, D. A. Sanders, D. Alves, R. Rodriguez, J. Dash, G. J. McKenzie, A. R. Venkitaraman and S. Balasubramanian, *Journal of the American Chemical Society*, 2011, **133**, 2658-2663.
178. R. Cebrián, E. Belmonte-Reche, V. Pirota, A. de Jong, J. C. Morales, M. Freccero, F. Doria and O. P. Kuipers, *Journal of medicinal chemistry*, 2021, **65**, 4752-4766.

179. E. Belmonte-Reche, M. Martínez-García, A. Guédin, M. Zuffo, M. Arévalo-Ruiz, F. Doria, J. Campos-Salinas, M. Maynadier, J. J. López-Rubio and M. Freccero, *Journal of medicinal chemistry*, 2018, **61**, 1231-1240.
180. U. Yildiz, I. Kandemir, F. Cömert, S. Akkoç and B. Coban, *Molecular Biology Reports*, 2020, **47**, 1563-1572.
181. U. Shankar, N. Jain, S. K. Mishra, T. K. Sharma and A. Kumar, *Frontiers in microbiology*, 2020, 1269.
182. Y. Nural, S. Ozdemir, O. Doluca, B. Demir, M. S. Yalcin, H. Atabey, B. Kanat, S. Erat, H. Sari and Z. Seferoglu, *Bioorganic Chemistry*, 2020, **105**, 104441.
183. Y.-J. Lu, X.-L. Guo, M.-H. Xu, W.-W. Chen, W.-L. Wong, K. Zhang and C.-F. Chow, *Dyes and Pigments*, 2017, **143**, 331-341.
184. S. Cai, W. Yuan, Y. Li, X. Huang, Q. Guo, Z. Tang, Z. Fang, H. Lin, W.-L. Wong and K.-Y. Wong, *Bioorganic & medicinal chemistry*, 2019, **27**, 1274-1282.
185. N. Sun, L. Ban, M. Li, Z. Fang, X. Li, W. Yao, J. Pan, Y. Lu, Z. Liu and W.-L. Wong, *Journal of Pharmacological Sciences*, 2018, **138**, 83-85.
186. K. Kasza, P. Gurnani, K. R. Hardie, M. Cámara and C. Alexander, *Advanced Drug Delivery Reviews*, 2021, **178**, 113973.
187. C. Sahli, S. E. Moya, J. S. Lomas, C. Gravier-Pelletier, R. Briandet and M. Hémadi, *Theranostics*, 2022, **12**, 2383.
188. A. Singh, A. Amod, P. Pandey, P. Bose, M. S. Pingali, S. Shivalkar, P. K. Varadwaj, A. K. Sahoo and S. K. Samanta, *Biomedical Materials*, 2022, **17**, 022003.
189. G. A. Naclerio and H. O. Sintim, *Journal of Medicinal Chemistry*, 2021, **64**, 7272-7274.
190. B. Parrino, D. Schillaci, I. Carnevale, E. Giovannetti, P. Diana, G. Cirrincione and S. Cascioferro, *European Journal of Medicinal Chemistry*, 2019, **161**, 154-178.
191. S. Nakayama, I. Kelsey, J. Wang and H. O. Sintim, *Chemical Communications*, 2011, **47**, 4766-4768.
192. M. Gentner, M. G. Allan, F. Zaehringer, T. Schirmer and S. Grzesiek, *Journal of the American Chemical Society*, 2012, **134**, 1019-1029.
193. T. Seviour, F. R. Winnerdy, L. L. Wong, X. Shi, S. Mugunthan, Y. H. Foo, R. Castaing, S. S. Adav, S. Subramoni and G. S. Kohli, *npj Biofilms and Microbiomes*, 2021, **7**, 1-12.
194. I. Kelsey, S. Nakayama and H. O. Sintim, *Bioorganic & medicinal chemistry letters*, 2012, **22**, 881-885.
195. J. S. Madsen, O. Hylling, S. Jacquiod, S. Pécastaings, L. H. Hansen, L. Riber, G. Vestergaard and S. J. Sørensen, *The ISME journal*, 2018, **12**, 2330-2334.
196. T. Rasamiravaka, Q. Labtani, P. Duez and M. El Jaziri, *BioMed research international*, 2015, **2015**.
197. S. Nakayama, I. Kelsey, J. Wang, K. Roelofs, B. Stefane, Y. Luo, V. T. Lee and H. O. Sintim, *Journal of the American Chemical Society*, 2011, **133**, 4856-4864.
198. T.-F. Xuan, J. Liu, Z.-Q. Wang, W.-M. Chen and J. Lin, *Frontiers in microbiology*, 2020, **10**, 3163.
199. Y.-H. Zhang, X.-H. Huang, W.-L. Wong, J.-R. Luo, X.-C. Guo, W. Liu, J.-Q. Hou, M.-T. She, W.-H. Jiang and N. Sun, *Sensors and Actuators B: Chemical*, 2023, 132992.
200. T.-F. Xuan, Z.-Q. Wang, J. Liu, H.-T. Yu, Q.-W. Lin, W.-M. Chen and J. Lin, *Journal of Medicinal Chemistry*, 2021, **64**, 11074-11089.
201. D.-G. Ha and G. A. O'Toole, *Microbiology spectrum*, 2015, **3**, 3.2. 27.
202. J. Cheng, A. Torkamani, Y. Peng, T. M. Jones and R. A. Lerner, *Proceedings of the National Academy of Sciences*, 2012, **109**, 10827-10831.
203. X. Shao, W. Zhang, M. I. Umar, H. Y. Wong, Z. Seng, Y. Xie, Y. Zhang, L. Yang, C. K. Kwok and X. Deng, *MBio*, 2020, **11**, e02926-02919.
204. R. K. Moyzis, J. M. Buckingham, L. S. Cram, M. Dani, L. L. Deaven, M. D. Jones, J. Meyne, R. L. Ratliff and J.-R. Wu, *Proceedings of the National Academy of Sciences*, 1988, **85**, 6622-6626.
205. G. N. Parkinson, M. P. Lee and S. Neidle, *Nature*, 2002, **417**, 876-880.
206. A. Verma, K. Halder, R. Halder, V. K. Yadav, P. Rawal, R. K. Thakur, F. Mohd, A. Sharma and S. Chowdhury, *Journal of medicinal chemistry*, 2008, **51**, 5641-5649.

207. A. Verma, V. K. Yadav, R. Basundra, A. Kumar and S. Chowdhury, *Nucleic acids research*, 2009, **37**, 4194-4204.
208. J. Hilton, K. Gelmon, P. L. Bedard, D. Tu, H. Xu, A. V. Tinker, R. Goodwin, S. A. Laurie, D. Jonker and A. R. Hansen, *Nature communications*, 2022, **13**, 1-12.
209. C. V. Dang, E. P. Reddy, K. M. Shokat and L. Soucek, *Nature Reviews Cancer*, 2017, **17**, 502-508.
210. D. Nejman, I. Livyatan, G. Fuks, N. Gavert, Y. Zwang, L. T. Geller, A. Rotter-Maskowitz, R. Weiser, G. Mallel and E. Gigi, *Science*, 2020, **368**, 973-980.

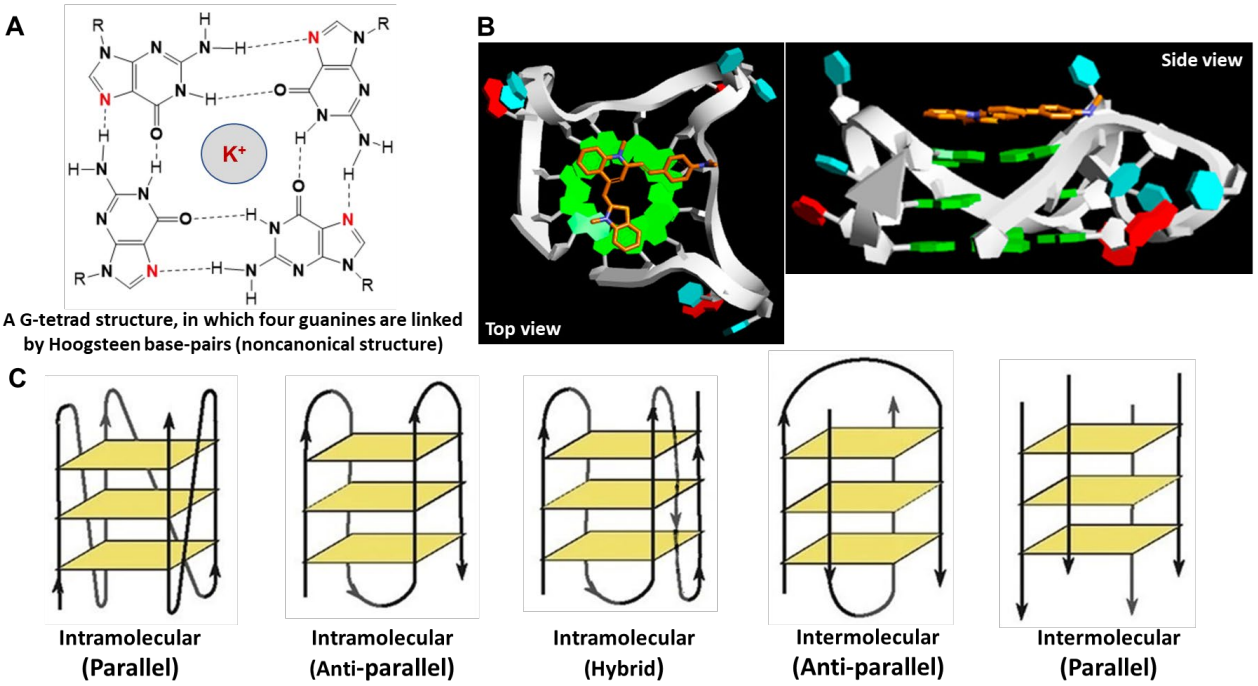

Figure 1. (A) A noncanonical G-tetrad structure in which four guanines are linked by Hoogsteen base-pairs and stabilized with a potassium ion. The R group can be ribose or deoxyribose. (B) A model of a Telo21 G-quadruplex in complex with a ligand: Top view showing the upper G-tetrad and side view showing the stacked tri-tetrad structure. Adapted with permission from ref. 84. Copyright (2016) American Chemical Society. (C) A schematic to present the topology of G4s folded into different conformations with different number of nucleic acid strands.

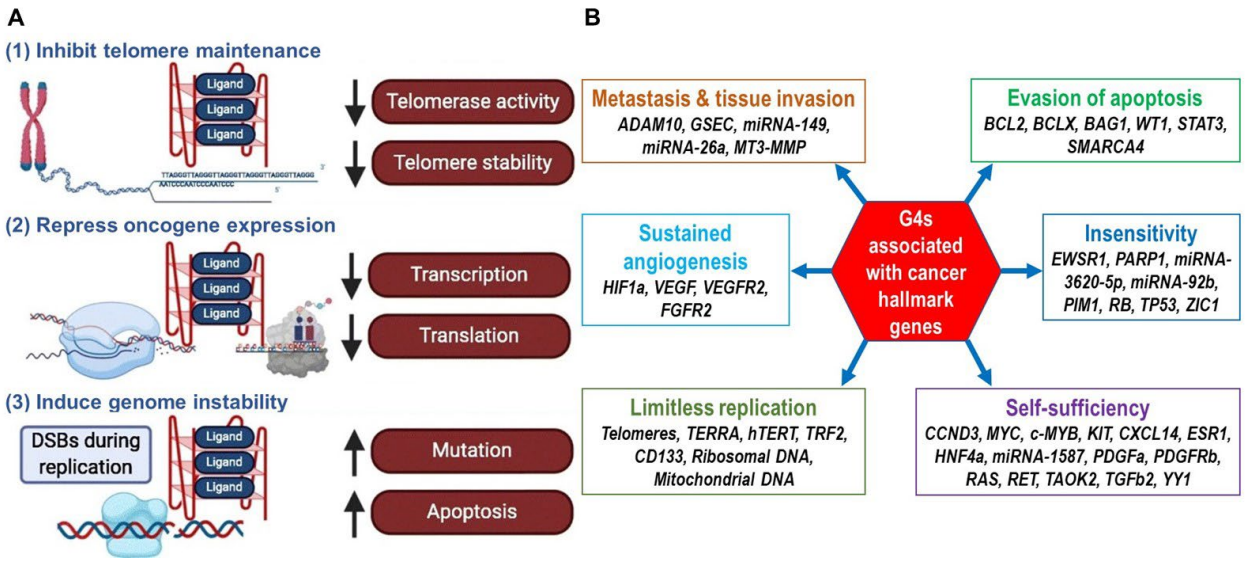

Figure 2. (A) A schematic to present the effects of ligands on the induction and/or stabilization of G4s in human cancer cells. G4-ligands are designed to inhibit the proliferation of cancer cells. The growth inhibition is most likely the consequence of alteration within biological processes. Depending on the ligand and cell type, the stabilization of G4-structures with the ligand interacted may result in changes in (1) a telomere maintenance, (2) gene expression of oncogenes and (3) increased genome instability.[76] (B) Some typical G4-hallmarks of cancer found in cancer-promoting genes. Each of these G4-hallmarks may show different cellular functions in cancer cells such as metastasis and tissue invasion, evasion of apoptosis, insensitivity, self-sufficiency, limitless replication, and sustained angiogenesis. In addition, the intramolecular G4s may exhibit great conformational diversity and differ by folding pattern, number of tetrads, loop size and constituent bases.[87]

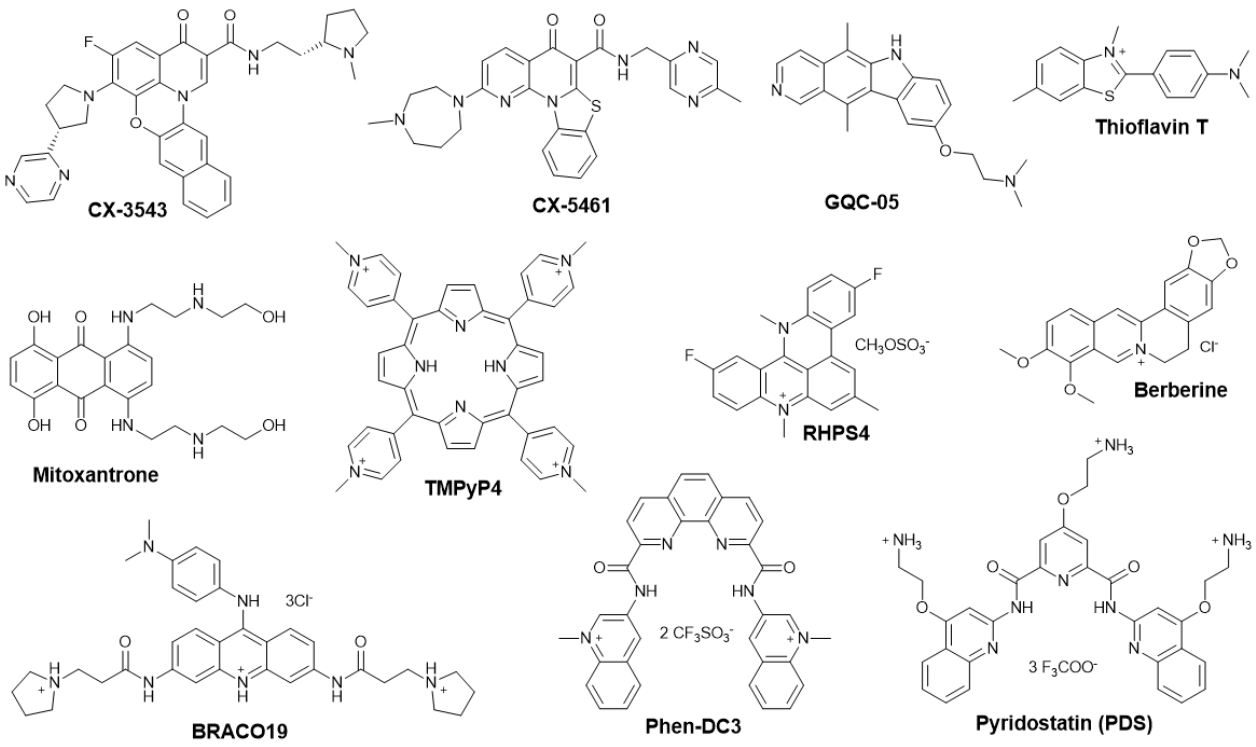

Figure 3. Some representative bioactive G4-ligands bearing a planar molecular fragment and positively charged.

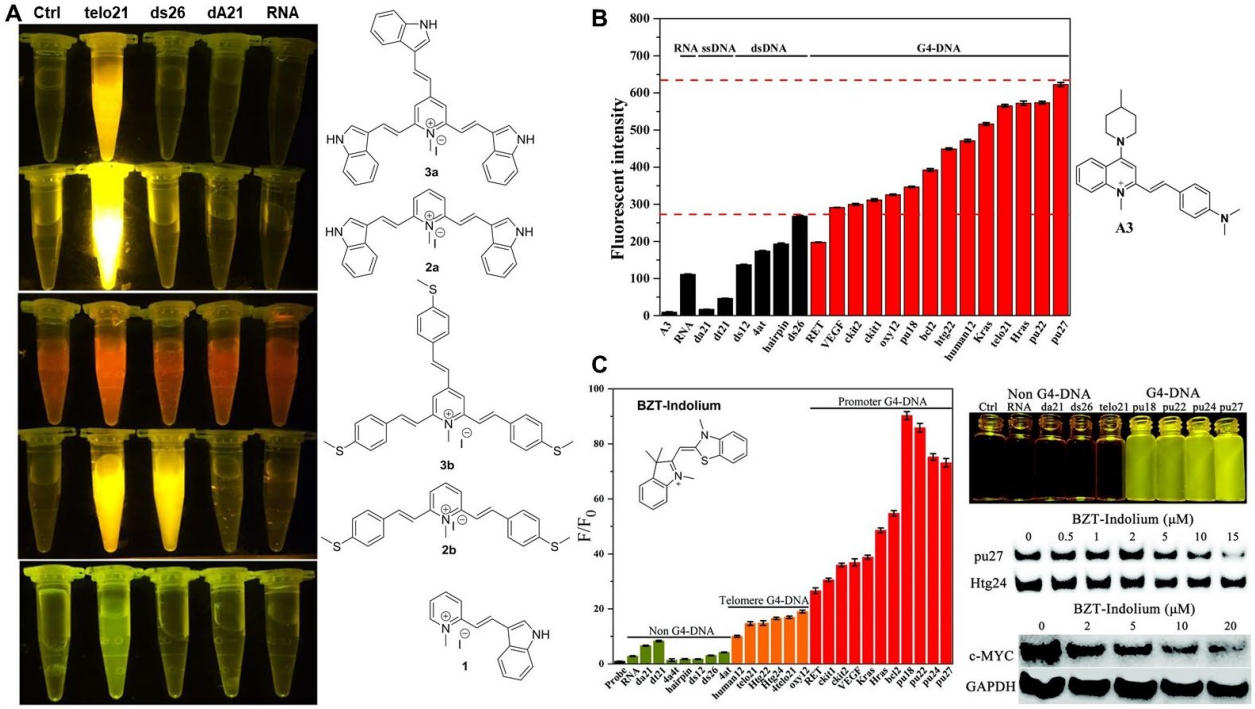

Figure 4. (A) The fluorescence changes of ligands, **1**, **2a–b** and **3a–b** (λ_{ex}=302 nm) with the presence of various nucleic acids:[118] G-quadruplex telo21, double-stranded DNA ds26, single-stranded DNA dA21 and RNA in a 10 mM Tris-HCl, 60 mM KCl, pH 7.4 buffer solution. Adapted with permission from ref. 118. Copyright (2016) Elsevier B.V. (B) A new molecular design based on the 1-methylquinolinium scaffold to develop near-infrared fluorescence probe (**A3**, λ_{ex}=498, λ_{em}=610, Stokes shift=112 nm, Φ_f=0.56).[126] The integration of a rotatable terminal amino group to 1-methylquinolinium results in high selective toward G4-DNA substrates. Adapted with permission from ref. 123. Copyright (2020) Elsevier B.V. (C) A small-sized fluorescent BZT-Indolium based G4-binding ligand was demonstrated as a highly selective and photostable sensor for *in vitro* staining and live cell imaging targeting c-MYC promoter G4-DNA. It was found to be able to inhibit the amplification of the c-MYC G-rich G4-sequence and down-regulate oncogene c-MYC expression in human cancer cells (HeLa).[125]

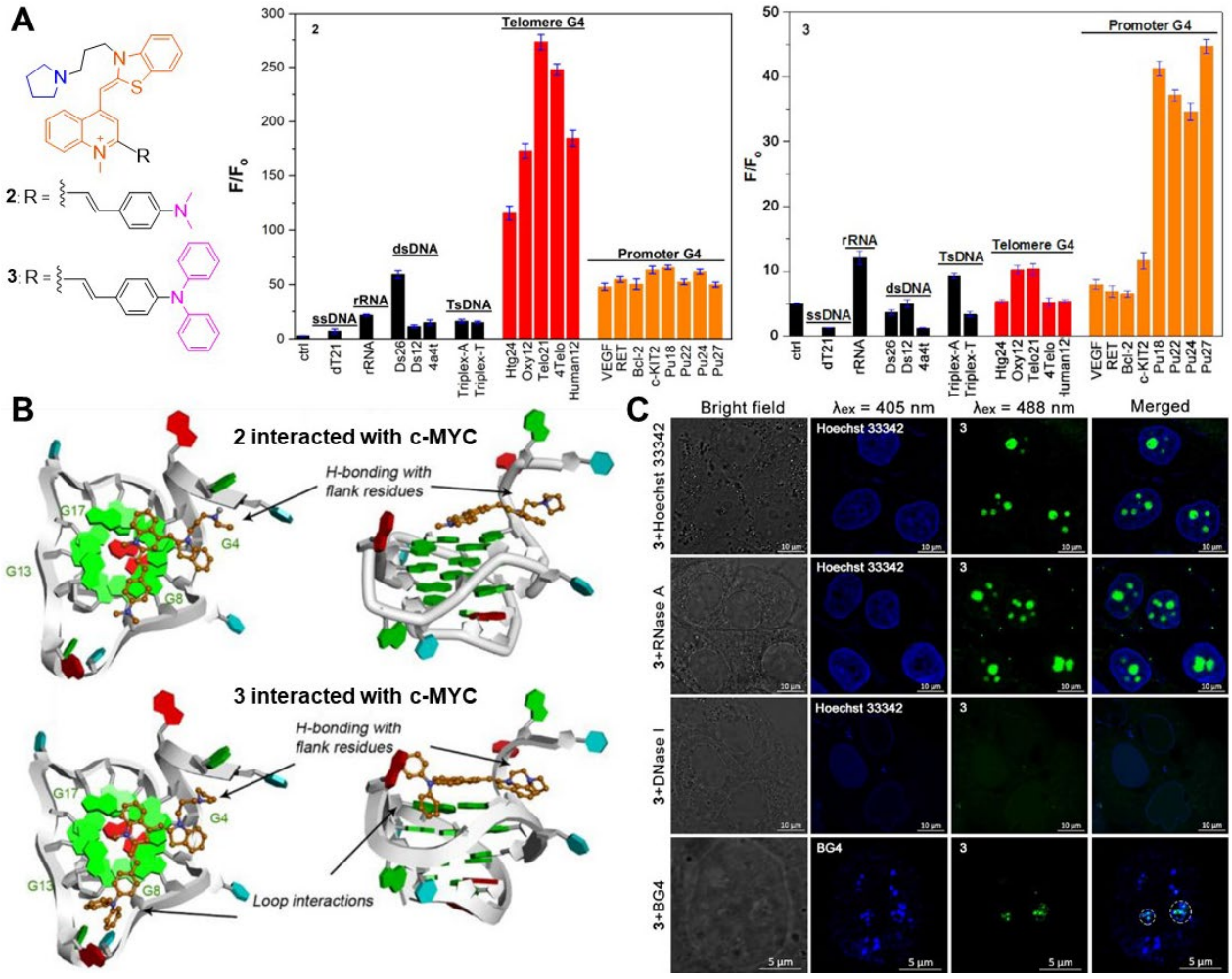

Figure 5. (A) The highly selective G4-ligands modified from a thiazole orange scaffold provide two-directional and multi-site interactions with the flanking residues and loops of the G4-motif. Ligand **2** is targeting telomeric G4-DNA structures and **3** is targeting c-MYC G4-DNA structures.[81] (B) Molecular docking study predicts that ligand **3** has its two terminal phenyl rings interacting with loop residues of c-MYC pu27 G4 (PDB 2MGN) while **2** does not have loop interactions. (C) Cell imaging and BG4 co-colocalization studies with ligand 3 in MCF-7 cells.[81]

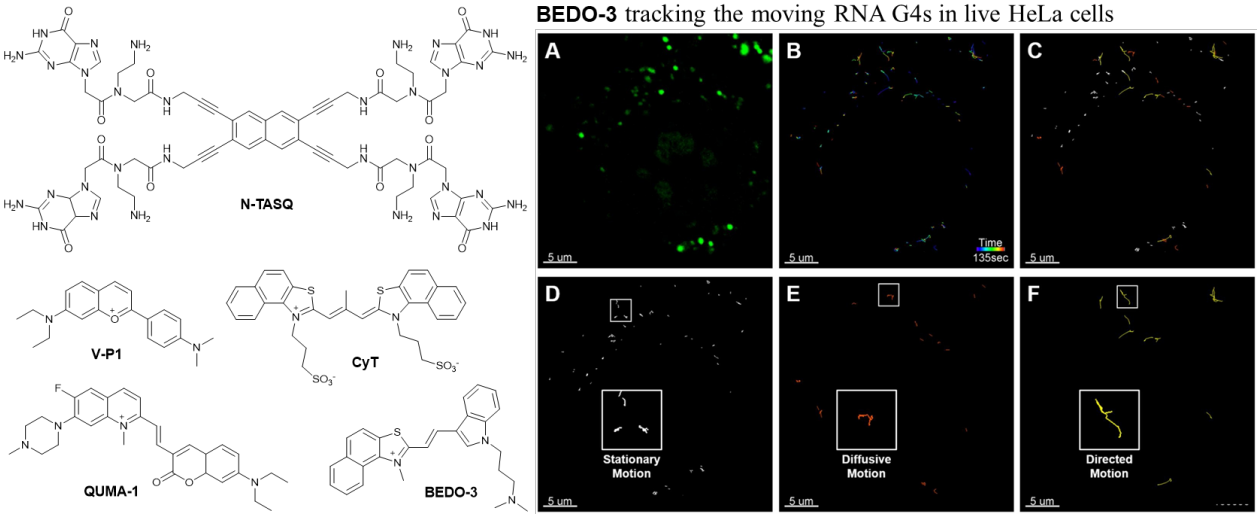

Figure 6. The reported RNA G4-selective fluorescent ligands and the study of **BEDO-3** in tracking the movements of RNA G4s in live HeLa cells: (A) Confocal fluorescence images of live cells stained with the probe. (B) Mobility analysis of the foci in (A); (C-F) Classification of motion types of the foci. Representative trajectories of the foci showing stationary (D), diffusive (E), and directed (F) motions. Reprinted with permission ref. 145. Copyright (2020) Elsevier B.V.

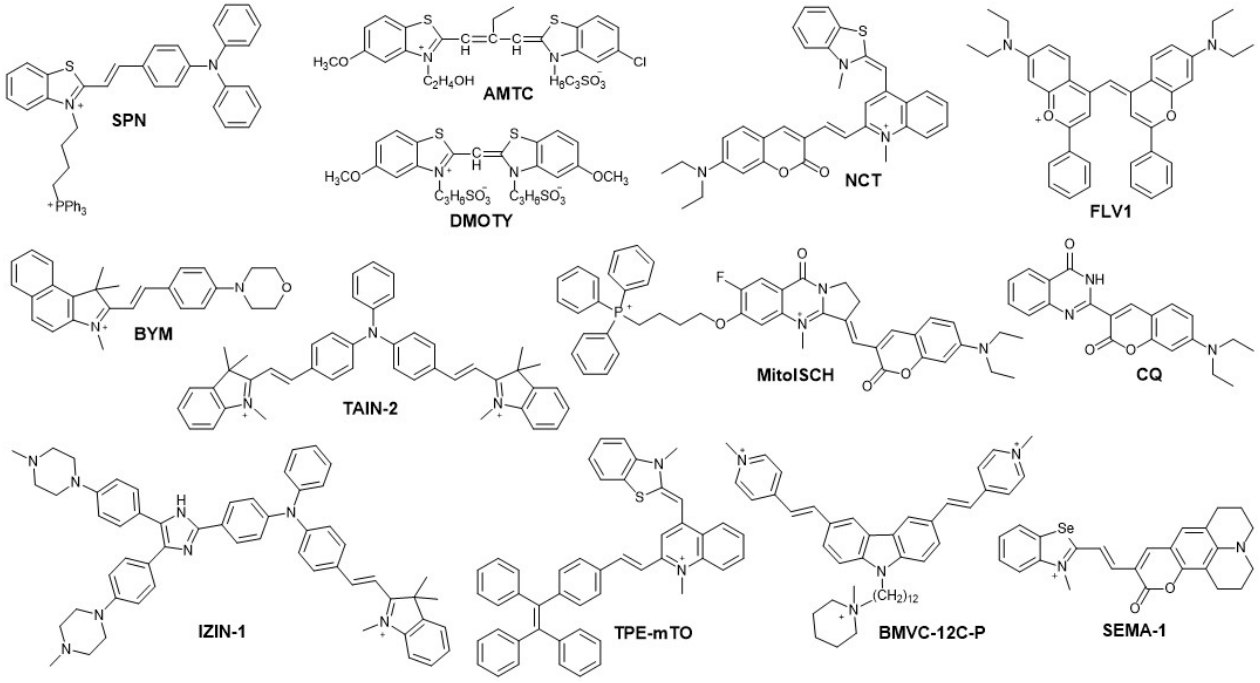

Figure 7. The fluorescent ligands with high selectivity toward mtDNA G4s against other nucleic acid structures *in vitro* and in live cells.

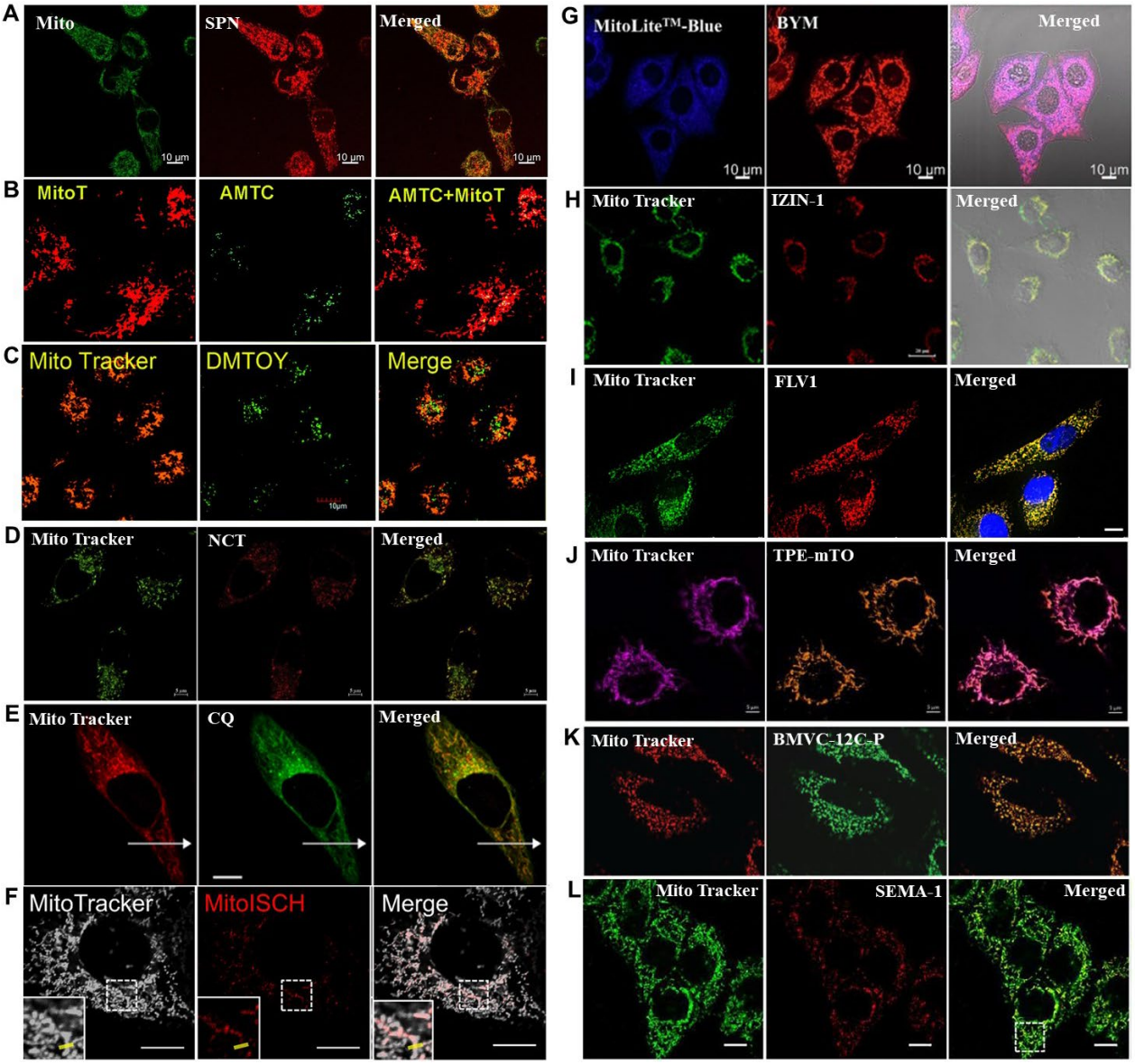

Figure 8. Confocal fluorescence images of mitochondria stained with different mtDNA G4 probes in live cells. (A) **SPN** (λ_{ex}: 561 nm, 20 μM) and Mito-Tracker ((λ_{ex}: 488 nm, 0.2 μM) in HeLa cells; scale bar: 10 μm.[154] (B) **AMTC** (λ_{ex}: 559 nm, 2 μM) and MitoTracker Deep Red (λ_{ex}: 633 nm, 50 nM) in HeLa cells.[155] (C) **DMTOY** (λ_{ex}: 405 nm, 10 μM) and MitoTracker Deep Red (λ_{ex}: 633 nm, 50 nM) in HeLa cells; scale bar: 10 μm.[156] (D) **NCT** (λ_{ex}: 488 nm, 1 μM) and Mito Tracker green (λ_{ex}: 488 nm, 1 μM) in HeLa cells; scale bar: 5 μm.[157] (E) **CQ** (λ_{ex}: 488 nm, 2 μM) and MitoTracker Red CMXRos (λ_{ex}: 561 nm, 0.2 μM) in HepG2 cells; scale bar: 10 μm.[158] (F) **MitoISCH** (λ_{ex}: 560 nm, 1 μM) and MitoTracker Green (λ_{ex}: 488 nm, 0.4 μM) in HeLa cells; scale bar: 10 μm.[161] (G) **BYM** (λ_{ex}: 530 nm, 5 μM) and MitoLite™-Blue (λ_{ex}: 488 nm, 1 μM) in HeLa cells; scale bar: 10 μm.[128] (H) **IZIN-1** (λ_{ex}: 543 nm, 4 μM) and MitoTracker™ Green (λ_{ex}: 488 nm, 0.1 μM) in A549 cells; scale bar: 20 μm.[163] (I) **FLV1** (λ_{ex}: 643 nm, 0.2 μM) and MitoTracker Green (λ_{ex}: 488 nm, 0.25 μM) in HeLa cells; scale bar: 5 μm.[164] (J) **TPE-mTO** (λ_{ex}: 488 nm, 1 μM) and Mito Tracker Deep Red (λ_{ex}: 633 nm, 1 μM) in A549 cells; scale bar: 5 μm.[165] (K) **BMVC-12C-P** (5 μM) and Mito Tracker Red (20 nM) in HeLa cells.[166] (L) **SEMA-1** (λ_{ex}: 640 nm, 1 μM) and MitoTracker Green (λ_{ex}: 488 nm) in live HeLa cells; scale bar: 10 μm.[167]

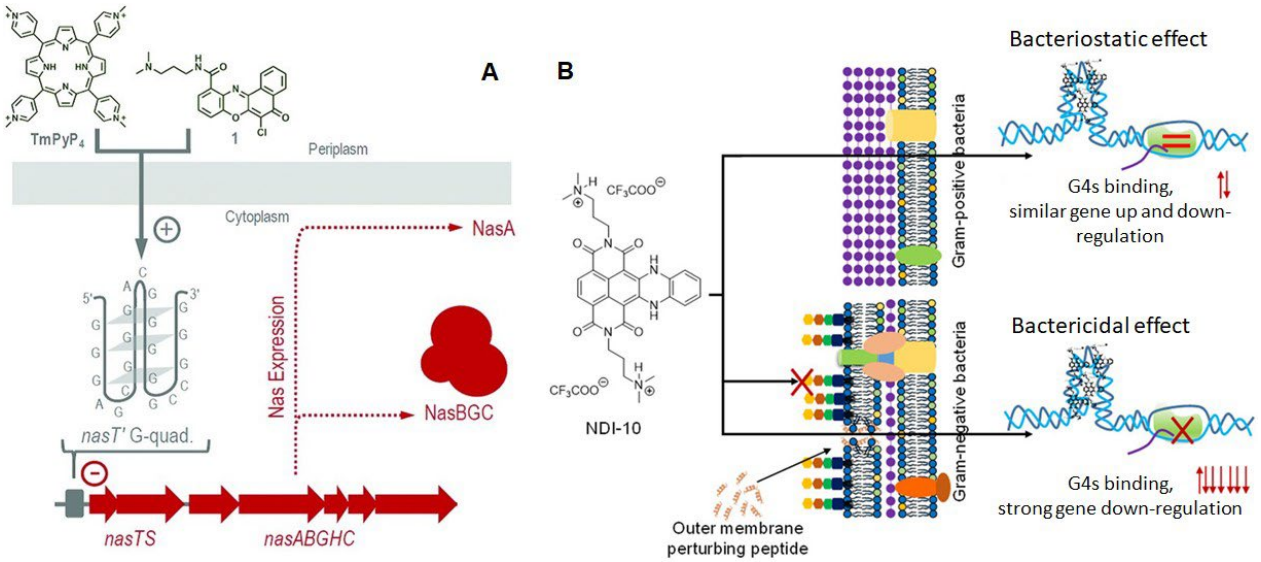

Figure 9. (A) A proposed mechanism for **TmPyP4** and **1** in control of Nas-dependent growth of *P. denitrificans:* (i) (+) stabilization of the G4 of *nasTS* and (ii) (-) inhibition of *nas* transcription.[174] (B) A G4-ligand **NDI-10** was proposed to show two different mechanisms in killing Gram-positive or negative bacteria. The ligand may exert its function on gene expression by targeting the bacterial G4s with different roles such as promoting transcription in Gram-positive bacteria and repressing transcription in Gram-negatives.[178]

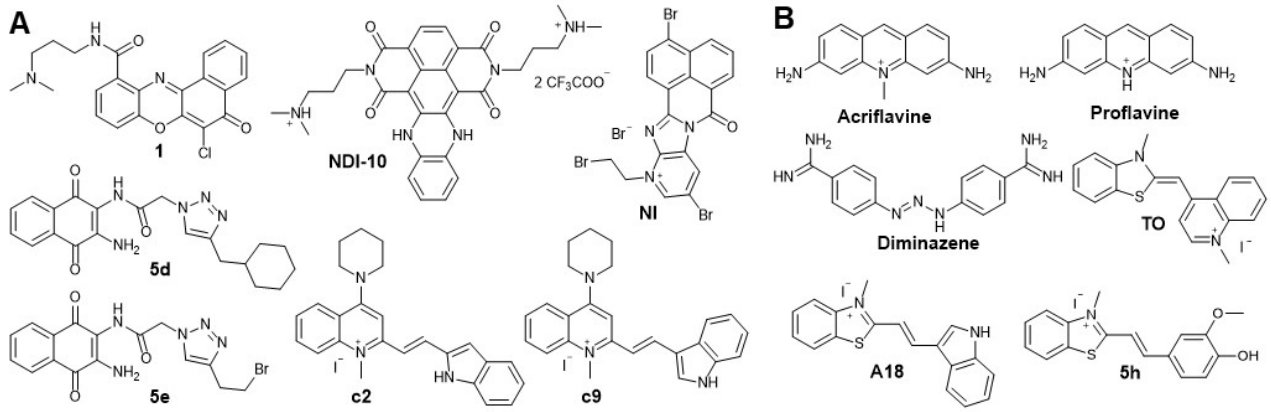

Figure 10. The recent reported G4-binding ligands: (A) for antibacterial study; (B) for bacterial biofilm formation eradication.

Table of Contents Entry

The recent advances of G-quadruplex-selective ligands in the fields of live cell imaging, chemical biology and therapeutic prospects against bacterial infections.